university of groningen

University Medical Center Groningen

University of Groningen

The distribution of Fe in the Antarctic Circumpolar Current

Löscher, B.M.; Baar, H.J.W. de; Jong, J.T.M. de; Veth, C.; Dehairs, F.

Published in:
Deep Sea Research Part II: Topical Studies in Oceanography

DOI:
10.1016/S0967-0645(96)00101-4

IMPORTANT NOTE: You are advised to consult the publisher's version (publisher's PDF) if you wish to cite from it. Please check the document version below.

Document Version
Publisher's PDF, also known as Version of record

Publication date:
1997

Link to publication in University of Groningen/UMCG research database

Citation for published version (APA):
Löscher, B. M., Baar, H. J. W. D., Jong, J. T. M. D., Veth, C., & Dehairs, F. (1997). The distribution of Fe in the Antarctic Circumpolar Current. *Deep Sea Research Part II: Topical Studies in Oceanography*, *44*(1), 143-187. https://doi.org/10.1016/S0967-0645(96)00101-4

Copyright
Other than for strictly personal use, it is not permitted to download or to forward/distribute the text or part of it without the consent of the author(s) and/or copyright holder(s), unless the work is under an open content license (like Creative Commons).

The publication may also be distributed here under the terms of Article 25fa of the Dutch Copyright Act, indicated by the “Taverne” license. More information can be found on the University of Groningen website: https://www.rug.nl/library/open-access/self-archiving-pure/taverne-amendment.

Take-down policy
If you believe that this document breaches copyright please contact us providing details, and we will remove access to the work immediately and investigate your claim.

Downloaded from the University of Groningen/UMCG research database (Pure): http://www.rug.nl/research/portal. For technical reasons the number of authors shown on this cover page is limited to 10 maximum.

Download date: 05-05-2023

Pergamon

PII: S0967-0645(96)00101-4

Deep-Sea Research II, Vol. 44, No. 1-2, pp. 143-187, 1997
© 1997 Elsevier Science Ltd
Printed in Great Britain. All rights reserved
0967-0645/97 $17.00 + 0.00

The distribution of Fe in the Antarctic Circumpolar Current

B. M. LÖSCHER,* H. J. W. DE BAAR,* J. T. M. DE JONG,* C. VETH* and F. DEHAIRS†

(*Received* 12 *September* 1995; *in revised form* 13 *September* 1996; *accepted* 22 *September* 1996)

Abstract—The large-scale distributions of dissolved and total Fe in surface and deep waters of the Antarctic Circumpolar Current exhibit strong relationships with hydrography and biological processes. The mean dissolved Fe concentrations are low in surface waters of the Antarctic Circumpolar Current (0.31–0.49 nM, with a minimum of 0.17 nM) and higher (averaging 1.1–1.9 nM) in the Polar Frontal region. Enhanced dissolved surface water concentrations in the Polar Frontal region are attributed to input from the continental shelf and coincide with phytoplankton spring blooms of large diatoms. The effects of sea-ice melting and iceberg melting on the Fe concentrations were relatively small.

Dissolved deep-water concentrations (> 400 m) in the Antarctic Circumpolar Current ranged from 0.4 to 2.8 nM. Circumpolar Deep Water has relatively high dissolved Fe concentrations in the Polar Frontal region (0.4–2.8 nM) compared with deep waters further to the south (0.6–1.1 nM). Similarly, total dissolvable (unfiltered) Fe concentrations in the Upper Circumpolar Deep Water tend to decrease southward from the Polar Frontal region. In the Lower Circumpolar Deep Water total dissolvable Fe concentrations are higher than in the Upper Circumpolar Deep Water due to the existing nepheloid layer and sources on the Mid-Atlantic Ridge. Dissolved and total dissolvable Fe concentrations in the Antarctic Bottom Water are higher than those of other water masses in the Antarctic Circumpolar Current, consistent with the nepheloid layer as well as diagenetic input from shelf sediments.

The High-Nutrient/Low-Chlorophyll areas of the Antarctic Ocean and northeast Pacific Ocean have different major Fe input sources of similar magnitude. In the Antarctic Circumpolar Current upward transport of Fe is the main input source, whereas in the North Pacific Ocean, aerosols are the dominant source. © 1997 Elsevier Science Ltd. All rights reserved

INTRODUCTION

Iron is a remarkable chemical element, with a very high abundance in the continental crust (Taylor, 1964), but extremely low concentrations in modern oxygenated seawater (Gordon *et al.*, 1982; Landing and Bruland, 1987; Saager *et al.*, 1989; Martin *et al.*, 1989, 1990a, 1993). The primordial ocean, under an oxygen-free atmosphere, likely had very high concentrations of reduced dissolved Fe(II), readily available for incorporation in biota during the first stages of biological evolution (Staley and Orians, 1992). This has led to Fe having several key functions in all known modern biota. For example the similar high availability of dissolved sulphide S(II) in the ancient oceans, now appears to be consistent with the ubiquity of the Fe–S-rich ferredoxin in all biological systems (Wächtershäuser, 1992; Russell *et al.*, 1993). However, largely because of photosynthesis, an oxygenated atmosphere and ocean evolved where Fe is very unstable in solution as it tends to precipitate

* Netherlands Institute for Sea Research, P.O. Box 59, 1790 AB Den Burg (Texel), The Netherlands.
† Analytische Chemie, Vrije Universiteit Brussel, Pleinlaan 2, Brussels B-1050, Belgium.

out into solid Fe(III) phases. Consequently, in modern open-ocean waters the very low abundance of dissolved Fe may have become limiting for plant life itself. Nevertheless, in anaerobic marine sediments or semi-enclosed basins, high concentrations of dissolved Fe(II) are known to persist. Photochemical reduction also may lead to substantial concentrations of Fe(II) in surface waters (Waite *et al.*, 1995).

Continental inputs of Fe into the oceans occur via fluvial (Martin and Meybeck, 1979) and atmospheric pathways (Hodge *et al.*, 1978; Prospero, 1981; Moore *et al.*, 1984; Duce, 1986; Martin and Gordon, 1988; Duce and Tindale, 1991; Duce *et al.*, 1991; Zhuang *et al.*, 1992), while ice-rafting plays a role in polar regions (Martin *et al.*, 1990a; Nolting *et al.*, 1991; Westerlund and Öhman, 1991). However, most of this land-derived material is highly refractory and remains in the particulate form with little alteration, eventually depositing in deep sea sediments, e.g. the aeolian red clay sediments of the central gyres. Also, the rather high dissolved Fe in river waters largely flocculates out in estuaries (Sholkovitz, 1978). Apart from continental input, dissolved Fe(II) diffuses out of reducing marine sediments (Kremling and Peterson, 1978; Murray and Gill, 1978; Froelich *et al.*, 1979). This, in combination with resuspension of particulate Fe contributes to the existence of nepheloid layers (Symes and Kester, 1985; Hong and Kester, 1986). Hydrothermal input discharging at the ridge axis is the major source for Fe and other metals in metalliferous sediments depositing on Mid-Ocean Ridges (Heath and Dymond, 1977; Rona *et al.*, 1984; von Damm *et al.*, 1985a,b; Hudson *et al.*, 1986; Thompson *et al.*, 1988). Obviously the overall input of dissolved Fe into open ocean waters is extremely low, most notably in the Antarctic Ocean where the aeolian and riverine input are smallest.

From thermodynamic considerations (Stumm and Morgan, 1981; Byrne *et al.*, 1988), dissolved Fe is expected to become oxidised into insoluble oxyhydroxides in oxygenated seawater. Hence Fe and other redox metals (e.g. Mn, Ce, Co) may disappear rapidly by oxidative scavenging. However, in oligotrophic oceanic regions with an extremely low abundance of biogenic particles, the residence time of dissolved Fe still may be significant.

Most of the dissolved Fe, i.e. that fraction that passes through a filter with 0.2 or 0.4 μm pore size, may well be present as colloids (Wells and Mayer, 1991). Obviously iron exists in a variety of physicochemical forms, where filtration serves only as an operationally defined cut-off in the continuum from true solution to real particles (Wells *et al.*, 1995). Even for the truly dissolved phase, it has been estimated that more than 99% of the Fe may be bound to natural organic complexing ligands (van den Berg, 1995; Rue and Bruland, 1995). This would greatly affect the assimilation rate by phytoplankton. In the current study, neither colloids nor dissolved organic moieties have been assessed. The measured dissolved Fe, as defined by the 0.4 μm nominal pore size of membrane filters, is taken to be the relevant variable for biological processes.

Iron is an essential element for phytoplankton growth, hence overall oceanic productivity. It is a key element in the respiratory electron transport chains (Raven, 1988), and is essential in the synthesis route of chlorophyll (Chereskin and Castelfranco, 1982). It is also required for the reduction of nitrate and nitrite (Timmermans *et al.*, 1994; van Leeuwe *et al.*, 1997; de Baar *et al.*, 1997) needed for the production of amino acids for incorporation into proteins. With respect to the Antarctic Ocean, it has been suggested that the growth of plankton might be limited due to a low input of Fe into surface waters (Gran, 1931; Martin and Fitzwater, 1988; de Baar, 1994). This would be one explanation for the "Antarctic paradox", that is, why the ocean around Antarctica has such high concentrations of the major nutrients nitrate, phosphate and silicate, but nevertheless low primary production.

Several factors conceivably limiting algal growth have been hypothesised (Cullen, 1991; Lancelot *et al.*, 1993), of which the most important are:

— light limitation of phytoplankton growth because of the great mixing depth, low insolation during winter, sea-ice cover and cloud cover (Cullen *et al.*, 1992);
— grazing control as a loss term of the plankton (Walsh, 1976; Wheeler and Kokkinakis, 1990; Frost, 1991) and
— limiting concentrations of Fe (Gran, 1931; Martin *et al.*, 1990a,b; Martin, 1991, 1992).

Although these explanations have sometimes been regarded as alternatives, it is obvious that different factors always act simultaneously (Hart, 1934, 1942; de Baar *et al.*, 1989, 1990; de Baar, 1994), albeit differently for separate parts of the algal size-spectrum, also in relation to size and succession of zooplankton grazers (Buma *et al.*, 1991; Riegman *et al.*, 1993). At present, it appears that light limitation, combined with intense grazing, controls the biomass of small algae, which by predominantly growing on recycled ammonia would have an approximately 40% lower cellular iron requirement (Raven, 1990). Obviously the success of large algae is just as well affected by light conditions, but the low availability of Fe appears to pose severe restrictions as well on the growth rate and biomass of the larger phytoplankton species, such as large diatoms. This is partly due to the role of Fe in nitrate- and nitrite-reductase (Price *et al.*, 1994; Timmermans *et al.*, 1994). Moreover, diffusion limitation generally restricts Fe-uptake by larger phytoplankton, which have a lower surface-to-volume ratio for diffusive transport rate versus rate of growth (Morel *et al.*, 1991; Hudson and Morel, 1993; Kiørboe, 1993).

Surface waters of the equatorial Pacific Ocean and the subArctic Pacific and Atlantic Oceans also exhibit appreciable concentrations of major nutrients nitrate, phosphate and silicate, albeit not nearly as high as in the Antarctic Ocean. These so-called High Nutrient, Low Chlorophyll (HNLC) regions contrast the central gyres of the temperate oceans, where depletion of major nutrients is common, and appear consistent with a generally very low biological productivity. The open waters of the Southern Ocean largely exhibit similar low productivity, i.e. are just as oligotrophic, but local "pulse areas" of enhanced productivity do exist (Holm-Hansen *et al.*, 1977; Sakshaug and Holm-Hansen, 1984; Heywood and Priddle, 1987; Smith and Sakshaug, 1990; Perisinotto *et al.*, 1992; Sullivan *et al.*, 1993). The location and season of such natural pulse areas may provide more insight into the production-limiting factors.

In the northeast Pacific and North Atlantic Oceans (Martin *et al.*, 1989, 1993), the very similar shape of vertical profiles of Fe and major nutrients, at first glance, suggests that Fe is strongly involved in the biological cycle, with presumably a fairly constant proportion of the major elements N, P and Si. However, these reported deep Fe concentrations are uniform at about 0.6 nM in both oceans, in contrast with the increasing concentrations of the nutrients and recycled trace metals (Cd, Zn, Cu, Ni), with increasing age of the deep Atlantic to deep Pacific waters (Boyle *et al.*, 1976, 1977, 1981; Sclater *et al.*, 1976; Bruland *et al.*, 1978a,b; Moore, 1978; Bruland, 1980; Bruland and Franks, 1983; Saager *et al.*, 1992; de Baar *et al.*, 1994). Various other data-sets also suggest any relation between dissolved Fe and plant nutrients (Symes and Kester, 1985; Landing and Bruland, 1987; Saager *et al.*, 1989; Nolting *et al.*, 1991) to be far from straightforward. Apparently, different water masses in various oceans have very different iron distributions due to different circulation and biogeochemistry. Most notably, the distribution of Fe within the ocean interior is dominated by redox-processes (Landing and Bruland, 1987; Saager *et al.*, 1989) and

particle reactive scavenging (Balistrieri *et al.*, 1981), as alluded to by Symes and Kester (1985): "However, since iron is chemically more reactive, one would expect the factors controlling the iron distribution to be more complex than those associated with silicate". In the Southern Ocean the major nutrients are not completely depleted in surface waters. Hence, there is no a priori expectation of a correlation between dissolved Fe and the major nutrients. Currently, reliable data sets of dissolved Fe are scarce. Contamination during sampling and extraction is still a critical problem for investigating the distribution of Fe in seawater.

In austral spring (October/November 1992), samples were collected to observe the distributions of dissolved as well as total Fe in surface (<400 m) and deep waters of the Antarctic Circumpolar Current (ACC) at station sites at each full degree latitude, along a ~1000 km line at the 6°W meridian. In addition, particulate material was collected in surface waters by filtration. Samples of sea-ice, surface snow and brine were collected in order to assess their potential Fe contribution to the surface water during melting. Deep waters were sampled, not only for the sake of determining the deep Fe distributions in the ACC, but also to allow assessment of upward transport in this largest upwelling system of the world ocean.

Upon a brief description of the hydrography, the concentrations of dissolved and total Fe in surface and deep waters of the ACC are reported, with a special emphasis on the Polar Frontal region. Then the various conceivable sources of Fe, for surface and deep waters, are evaluated in relation to the requirements for biological growth in compartments of the plankton ecosystem. Some of the findings have been summarised briefly elsewhere (de Jong *et al.*, 1994; de Baar *et al.*, 1995). Here, sampling methods and actual data are presented and treated in detail, including the deep water data and particulate Fe results. Other trace metals (dissolved Cd, Cu, Ni and Zn, as well as the metals in particulate matter) were also studied during ANT X/6 and will be presented in subsequent papers.

SAMPLING AND METHODS

Samples were collected during the austral spring, from 4 October to 25 November 1992, during the Joint Global Ocean Flux Study (JGOFS) Antarctic Ocean expedition ANT/X6 aboard R.V. *Polarstern* (Fig. 1). The first transect started at Punta Arenas (Chile) and followed the ACC eastward until the 6°W meridian was reached. There, consecutive north–south sections were investigated along the 6°W meridian from 47°S to 59°S, including the Polar Frontal region and the Weddell Sea Gyre. Between transects 5 (station 887–907) and 11 (station 930–969), on average 18 days passed, during which the development of a spring bloom could be followed (station locations and numbers according to Smetacek *et al.*, 1997).

Seawater samples were taken with precleaned GoFlo samplers (12 l) mounted either on a 10 mm kevlar hydrowire (40–400 m) or on an all-Teflon coated CTD/Rosette frame (>400 m). At each full degree, six samples were collected with kevlar wire at standard depths (40–60–100–150–200–400 m), corrected afterwards for wire angle, using an SIS pressure sensor at the deepest (400 m) sampler. Water deeper than 400 m was collected with the CTD/Rosette frame. Surface water samples (~10 m; unfiltered) were taken from a walking bridge extending 10 m beyond the bow of the slowly upwind steaming ship, using a 2 l GoFlo sampler on a small winch with 6 mm kevlar wire. Upon recovery, the sampler was wrapped in plastic bags, transferred into a Class-100 clean air laboratory van, and drained

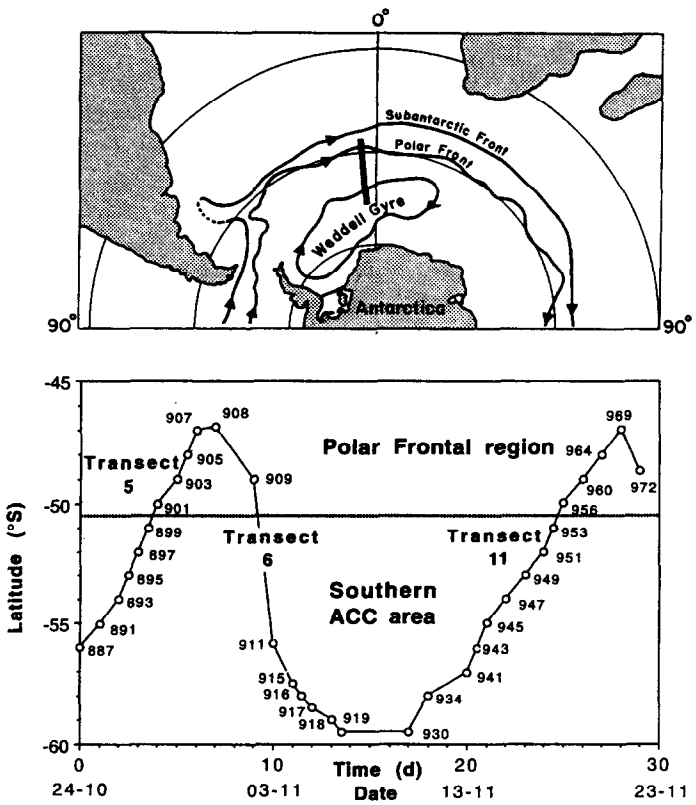

Fig. 1. Chart of the research area at the 6°W meridian extending from 47° to 59°S, crossing the Polar Front at about 49–50°S and the ACC–Weddell Gyre Boundary at about 58°S. The lower graph shows the latitude versus time (days) of the stations numbered 887 to 969 at consecutive transects 5/6 and 11, and Sta. 972 of transect 12. Not shown are the initial transects 1–4, and intermediate short transects 7–10, see Smetacek *et al.* (1997).

into a precleaned storage bottle. Particulate matter was collected by filtering 30–60 l of seawater through 142 mm Nuclepore filters with a 0.2 μm pore size. The seawater had been taken with a suite of 3–6 12 l GoFlo samplers on the CTD/Rosette frame.

Immediately upon recovery, the large 12 l GoFlo samplers were attached to the outside of the clean air laboratory van. Teflon tubes were connected to lead the seawater into the clean laboratory. Pressure lines, with high purity nitrogen gas passing over fine particle arrestance filters, were attached to the top of the samplers to allow for filtration by an overpressure of < 1 bar. Inside the clean laboratory, seawater was filtered over acid-cleaned Nuclepore or Poretics membrane filters (47 mm, 0.4 μm), mounted in all-Teflon (PTFE) filter holders. In addition, seawater samples were taken without filtering. The filtered or unfiltered seawater was collected into 1 or 2 l hot-acid-cleaned PE bottles, acidified to pH 2 with quartz-distilled HNO_3 and stored. Zhuang *et al.* (1990) reported an increasing dissolution of Fe in marine aerosols with decreasing pH of seawater. Hence, for the unfiltered samples it is assumed that the approximately 1 year storage at pH 2 would allow dissolution of at least some, if not most biogenic fractions and surface oxyhydroxide coatings. Only the most refractory

component of land-derived minerals (clays, sand, etc.) would still be excluded from the analysis.

At the ice stations, surface snow, ice and brine samples were collected using acid-cleaned plastic ware. The samples were placed in a laminar flow clean air bench for melting, then acidified, and transferred into PE bottles and stored.

In the clean laboratory onshore, the samples were pre-concentrated (167 ×) by an APDC/DDDC chloroform extraction in Teflon separatory funnels, according to Bruland and Franks (1979). The back extraction step was omitted. The extract was evaporated to dryness and the residue dissolved in diluted HNO_3. The reagents used were cleaned by 4-fold sub-boiling distillation in quartz stills. The final analyte was measured using a Perkin Elmer 5100 PC Graphite Furnace Atomic Absorption Spectrophotometer with Zeeman background correction.

In each daily session 18 samples and six blanks were extracted. Moreover, a suite of four spikes with increasing Fe concentrations was added to a three-times extracted seawater matrix to check the recovery of Fe. This was generally higher than 95%, as determined by linear regression. Results of extractions with recoveries of less than 90% were rejected, and are not reported. Seven examples of daily runs are listed in Table 1. The reproducibility of the overall analytical procedure, based on seven triplicates and 21 duplicates, ranged from 2 to 18%. For each daily run, the mean values for six blanks ranged between 0.09 and 0.22 nM. The detection limits, expressed as three times the standard deviation of the six daily blanks, ranged between 0.03 and 0.31 nM. In this manner about 200 samples were analysed in the 1993–1994 period. All values are reported and have been corrected for the corresponding daily mean blank and extraction efficiency.

In 1995 some stored samples of filtered seawater were re-analysed, using the very different Flow Injection Chemoluminescence method after Obata *et al.* (1993), yielding values in excellent agreement with earlier analyses. The reliability of the above described shipboard sampling with 12 l GoFlo at the 10 mm kevlar wire, and filtration, was recently confirmed in 1995–1996 expeditions in the Pacific and east Atlantic sectors, using the shipboard analyses after Obata *et al.* (1993) for final analyses. Very reproducible concentrations were found between various depths and stations (de Jong and de Baar, unpublished results).

Table 1. *Seven examples of six daily blanks, detection limits (*D.L. = *three times the standard deviation) and extraction efficiency with coefficient of correlation of linear regression for each period for Fe spike additions*

Date	17-03-93	10-06-93	18-06-93	22-06-93	15-10-93	30-11-93	18-12-93
Separatory funnel							
1	0.15	0.17	0.11	0.19	0.11	0.18	0.08
2	0.18	0.08	0.16	0.11	0.13	0.10	0.11
3	0.09	0.07	0.12	—	0.05	0.16	0.11
4	0.09	0.05	0.09	0.14	0.02	0.11	0.09
5	0.05	0.11	0.17	0.38	0.02	0.11	0.10
6	0.13	0.10	0.10	0.21	0.05	0.22	—
Average	0.12	0.10	0.12	0.21	0.06	0.15	0.10
D.L.	0.12	0.12	0.09	0.33	0.12	0.12	0.03
Extraction efficiency (%)	101	94	91	100	96	99	93
Coefficient of correlation	1.00	1.00	1.00	1.00	1.00	1.00	1.00

The particulate matter samples on 142 mm filters were subjected to a sequential chemical leaching treatment in the clean laboratory. They were immersed in 4.5 M Q-acetic acid for 4 h at room temperature to dissolve adsorbed cations, carbonate phases and reactive oxyhydroxides (Landing and Bruland, 1980, 1987). This was followed by a digestion in 2 M Q-HCl/1 M Q-HNO_3 again for 4 h at room temperature to dissolve the more resistant Fe(III) oxyhydroxides (Lewis and Landing, 1991). The residual refractory material was placed into clean digestion vessels and totally digested with 3 ml Q-HCl, 1 ml Q-HNO_3 and 1 ml ultraclean HF. After digestion in a microwave oven they were diluted with 5 ml of saturated H_3BO_3 to neutralise the strong acid HF (Merck). The last digestion step was tested for total destruction with the reference material calcareous loam (BCR no. 141) and light sandy soil (BCR no. 142) for the metals Cu and Ni. The obtained values agreed with the certified values within the 95% confidence interval. The blanks of Fe ranged between 0.43 and 5.67 pM, and between 0.07 and 1.07 nM for the acetic acid leaching step and the total destruction step, respectively. The blanks for the second leaching step were smaller than 0.01 nM. The detection limits, based on three times the standard deviation of the blanks, ranged between 1.57 and 3.15 pM, 0.6 and 7.8 pM, and 20 pM and 0.88 nM for the acetic acid leaching step, the second leaching step and the total destruction, respectively.

For the total particulate Al data, the seawater samples were collected independently by F. Dehairs in the upper 600 m using an all-Teflon coated CTD/Rosette frame with NOEX samplers. Typical depths were 10, 50, 100, 150, 200, 250, 300, 350, 425, 500 and 600 m. The seawater was transferred to 30-l acrylic (perspex) filtration units for filtration on Nuclepore membranes (47 mm, 0.4 μm porosity) using the pressure of filtered air. In general between 5 and 24 l of seawater were filtered per sample. After filtration, membranes were dried at 50°C and stored frozen in Millipore petri dishes until later analysis. At every station one blank membrane was dried and stored as carried out for the sample membranes. In the home laboratory filter samples were mineralised using a lithium metaborate ($LiBO_2$; Specpure, Johnson & Matthey) fusion technique as described by Dehairs *et al.* (1990, 1991). Prior to the fusion of the samples in platinum crucibles at 1100°C, the polycarbonate matrix of the membrane filters was gently combusted at 400°C. After fusion the samples were redissolved in hot (80°C) HNO_3 (Merck, Suprapure) under constant stirring. Final sample solution (10 ml) was 8% in HNO_3 and 5% in $LiBO_2$. Al was analysed by simultaneous inductively coupled plasma optical emission spectrometry (Jobin-Yvon 48). Standards were prepared in a similar $HNO_3/LiBO_2$ matrix as the samples.

The surface-water data for dissolved (filtered) and total dissolvable (unfiltered) Fe, as well as major nutrients are reported in Table 2. The deep-water data for hydrography, nutrients, filtered and unfiltered Fe are given in Table 3, and the total particulate Al data are reported in Table 4.

HYDROGRAPHY

Deep circulation

The hydrography has been described extensively by Veth *et al.* (1997). Briefly, the transects along the 6°W meridian from 47°S to 59°S (Fig. 1) extended to the north across the southern limits of North Atlantic Deep Water (NADW), which penetrates the ACC. Beyond 30°S the characteristics of NADW change due to mixing with overlying Antarctic

Table 2. Surface water stations of ANT X/6 with data on nutrients, dissolved and total dissolvable iron

Station/position/ date	Depth (m)	NO_3 (μM)	Si (μM)	PO_4 (μM)	Total Fe (nM)	Dissolved Fe (nM)
859	200	—	—	—	1.84	—
56°59′ S	300	—	—	—	1.54	—
38°51′ W						
04–10–92						
860	40	27.9	61.6	1.96	3.86	—
56°59′ S	100	33.2	68.7	1.97	3.28	—
30°27′ W	200	32.9	81.9	2.31	2.67	—
05–10–92	300	27.9	87.0	2.63	3.72	—
862	10	27.4	45.8	1.89	1.88	—
57°00′ S	40	27.5	45.8	1.87	—	1.25
23°19′ W	60	27.3	45.6	1.95	—	0.52
07–10–92	100	28.6	50.9	2.10	—	0.57
	150	28.6	51.1	1.95	—	0.42
	200	29.4	58.8	2.00	—	0.48
	300	35.5	75.6	2.45	—	0.77
865	40	27.9	42.4	1.91	—	0.59
56°09′ S	60	29.5	42.8	1.91	—	0.65
15°26′ W	100	28.5	42.1	2.40	—	0.42
09–10–92	140	28.5	42.8	1.95	—	0.50
	200	33.4	58.3	2.24	—	0.93
	300	35.8	80.0	2.45	—	1.33
866	100	33.9	91.5	2.26	2.15	—
57°45′ S	200	33.2	75.5	2.27	5.17	—
06°29′ W	300	31.9	74.5	2.36	3.44	—
11–10–92						
879	10	24.4	18.7	1.65	3.68	—
48°00′ S	37	24.8	18.7	1.65	1.55	0.52
06°00′ W	74	24.9	19.3	1.71	—	0.69
18–10–92	185	28.0	26.3	1.90	3.01	3.01
	277	32.5	44.0	2.27	—	1.66
887	38	27.6	48.7	1.84	—	1.48
55°59′ S	76	27.5	48.5	1.84	0.44	—
06°04′ W	95	28.1	48.2	1.86	0.39	—
24–10–92	142	30.9	56.9	2.40	0.69	—
	189	33.1	68.1	2.22	—	1.43
	284	34.8	82.8	2.32	1.02	—
891	10	27.1	39.9	1.76	5.55	—
55°01′ S	40	27.1	40.1	1.79	0.53	0.42
06°00′ W	60	27.1	40.5	1.78	—	0.37
25–10–92	150	28.6	44.5	1.87	—	0.42
	200	31.3	53.4	2.50	3.02	1.17
	300	35.0	77.3	2.32	—	0.90

(*Continued*)

Table 2. Continued

Station/position/ date	Depth (m)	NO_3 (μM)	Si (μM)	PO_4 (μM)	Total Fe (nM)	Dissolved Fe (nM)
893	10	26.8	41.5	1.87	7.39	—
54°00′ S	39	26.9	41.7	1.85	1.54	0.37
06°01′ W	59	26.9	41.9	1.86	—	0.38
26–10–92	99	27.0	42.1	1.86	—	0.22
895	10	26.5	36.3	1.82	2.03	—
53°00′ S	33	26.8	36.3	1.89	0.51	—
06°00′ W	123	27.2	37.0	1.90	—	0.77
26–10–92						
897	10	26.5	28.4	1.83	2.05	—
52°00′ S	40	26.7	28.6	1.90	1.34	1.15
06°00′ W	100	26.7	28.8	1.81	—	0.39
27–10–92	150	28.9	36.8	1.98	—	0.81
	200	34.2	59.3	2.29	3.44	0.34
	300	35.5	77.1	2.42	—	0.38
899	40	26.4	28.7	1.88	5.81	0.17
51°00′ S	60	26.8	28.4	1.84	—	0.69
06°00′ W	100	26.6	29.3	1.87	—	0.83
27–10–92	150	27.1	31.2	1.90	—	0.18
	200	30.5	43.5	2.15	2.68	0.47
	300	36.2	73.1	2.50	—	1.25
901	10	25.5	18.9	1.63	4.37	—
50°00′ S	40	26.9	20.1	1.71	3.82	3.07
06°00′ W	60	26.1	20.2	1.72	—	1.13
28–10–92	100	26.6	22.2	1.80	—	1.68
	150	28.6	29.5	1.98	—	1.43
	200	30.8	38.5	2.13	1.23	0.66
903	10	24.1	11.5	1.17	2.11	—
49°00′ S	40	24.4	11.7	1.15	7.03	0.17
06°00′ W	60	24.5	11.9	1.21	—	1.42
29–10–92	150	26.5	26.6	1.87	—	2.29
	300	33.5	53.3	2.38	—	1.96
905	40	23.0	14.8	1.62	0.82	0.26
48°00′ S	60	24.0	17.0	1.71	—	2.51
06°00′ W	100	24.7	19.7	1.79	—	3.77
29–10–92	150	26.2	24.3	1.91	—	0.44
	200	27.7	29.3	2.40	4.01	0.38
	300	32.4	43.2	2.25	—	1.94
907	10	23.6	13.4	1.57	2.64	—
47°00′ S	34	23.7	13.2	1.57	5.29	—
06°00′ W	51	23.7	13.9	1.57	—	(6.20)
30–10–92	85	24.9	15.9	1.51	—	0.54
	128	26.4	23.7	1.86	1.30	1.20
	170	27.2	26.3	1.91	—	0.94

(Continued)

Table 2. Continued

Station/position/ date	Depth (m)	NO_3 (μM)	Si (μM)	PO_4 (μM)	Total Fe (nM)	Dissolved Fe (nM)
908	100	32.9	14.2	1.57	—	2.28
46°52′ S	200	28.2	25.3	1.99	—	1.76
05°43′ W	250	31.8	38.6	2.24	8.92	—
31–10–92						
915	10	27.4	59.1	1.91	8.54	—
57°29′ S	40	27.3	58.9	1.95	1.67	0.79
06°00′ W	60	27.6	59.4	1.92	—	0.39
04–10–92	150	31.9	76.4	2.28	—	0.50
	300	33.1	88.3	2.34	—	1.42
916	40	28.1	67.2	1.95	1.83	—
58°00′ S	150	28.6	78.7	2.30	—	0.43
06°00′ W						
04–11–92						
918	40	28.0	77.7	2.10	1.54	—
59°00′ S	60	27.8	78.3	1.99	1.92	—
06°00′ W	100	27.7	79.9	2.20	1.20	—
06–11–92	200	30.5	99.0	2.16	2.04	—
	300	33.1	117.0	2.35	2.24	—
919	40	27.2	76.9	2.60	2.42	—
59°29′ S	60	27.3	77.7	2.60	1.24	—
06°00′ W	100	29.3	78.8	2.80	1.05	—
06–11–92	150	32.4	10.7	2.36	1.38	—
930	0 (Zodiac)	28.1	78.2	2.70	0.67	—
59°30′ S	10	28.0	78.2	2.60	2.03	—
06°00′ W	40	28.0	77.2	2.80	0.57	—
10–11–92	60	27.8	76.8	2.90	0.75	—
	100	27.9	77.4	2.10	1.13	—
	150	32.9	102.9	2.37	0.76	—
	200	33.3	110.8	2.43	0.65	—
934	40	29.0	75.3	2.30	0.86	—
58°00′ S	60	29.4	75.8	2.12	1.14	—
06°01′ W	100	28.9	77.3	2.40	0.88	—
11–11–92	200	32.3	87.4	2.26	1.28	—
941	38	27.9	61.8	1.95	—	0.55
57°03′ S	57	28.0	61.7	1.93	—	0.25
06°01′ W	95	28.8	63.6	2.10	—	0.22
13–11–92	142	33.5	75.5	2.33	—	0.63
	190	34.3	83.4	2.41	—	0.34
	285	33.6	89.4	2.36	—	0.34
943	10	27.6	50.6	1.91	1.12	—
56°01′ S	40	27.3	50.1	1.88	—	0.24
06°00′ W	60	27.6	50.5	2.10	—	0.40

(Continued)

Table 2. Continued

Station/position/ date	Depth (m)	NO_3 (μM)	Si (μM)	PO_4 (μM)	Total Fe (nM)	Dissolved Fe (nM)
13–11–92	150	30.0	98.2	2.40	—	0.70
	200	32.8	70.3	2.24	—	1.23
	300	34.3	87.6	2.42	—	2.00
945	10	27.0	43.8	1.86	1.11	—
55°00′ S	40	27.1	43.1	1.89	—	0.04
06°01′ W	60	27.1	43.2	1.87	—	0.22
14–11–92	100	27.7	43.6	1.89	—	0.39
	200	31.8	58.2	2.23	—	1.49
	300	34.8	78.1	2.45	—	1.00
947	59	26.7	42.9	1.90	—	1.90
54°00′ S	98	26.9	42.5	1.87	—	1.23
06°00′ W	148	27.1	43.6	1.90	—	1.22
15–11–92	197	29.8	51.9	2.80	—	0.98
	296	34.8	76.5	2.49	0.81	—
	394	34.0	86.6	2.39	0.71	—
949	10	27.8	39.2	1.93	1.92	—
53°00′ S	40	27.7	38.5	1.87	—	0.30
06°00′ W	60	27.3	38.8	1.88	—	0.61
16–11–92	100	27.1	39.2	1.89	—	0.16
	150	28.5	41.9	1.99	—	0.32
	200	34.2	66.4	2.37	—	0.57
953	10	26.5	27.4	1.85	3.69	—
51°00′ S	40	26.7	27.2	1.86	0.66	—
06°01′ W	60	26.4	26.9	1.84	0.80	—
17–11–92	150	27.5	32.9	1.94	0.81	—
	200	31.2	44.1	2.13	0.71	—
956	10	23.6	4.8	1.30	5.57	—
49°59′ S	39	23.8	7.1	1.11	—	1.31
06°00′ W	98	25.3	14.4	1.38	—	0.35
18–11–92	147	28.1	28.4	1.95	—	1.90
	294	35.2	59.2	2.43	—	0.96
	392	35.9	72.7	2.50	—	0.95
960	10	23.9	7.9	1.19	0.58	—
49°00′ S	39	23.6	6.9	1.22	—	2.03
06°00′ S	58	23.5	7.6	1.28	—	1.43
19–11–92	97	25.9	19.9	1.71	—	0.26
	194	30.0	35.1	2.50	—	0.89
	291	35.3	56.6	2.36	—	1.24
964	10	19.8	1.3	1.28	1.13	—
48°00′ S	40	21.0	3.9	1.50	—	2.65
06°00′ W	60	23.4	10.4	1.64	—	0.31
20–11–92	100	26.1	18.0	1.86	—	1.13
	200	30.1	28.4	2.80	—	1.29

(Continued)

Table 2. Continued

Station/position/ date	Depth (m)	NO_3 (μM)	Si (μM)	PO_4 (μM)	Total Fe (nM)	Dissolved Fe (nM)
	300	32.7	40.8	2.29	—	0.80
969	10	19.2	1.3	1.21	1.13	—
46°59′ S	40	20.2	1.0	1.29	0.49	—
06°00′ W	60	21.6	4.5	1.45	4.02	—
21–11–92	100	24.7	13.7	1.78	1.00	—
	200	29.5	24.5	2.00	2.80	—
	300	32.4	36.5	2.16	4.32	—
972	10	19.1	2.8	1.28	2.44	—
48°41′ S	39	20.8	4.4	1.32	—	2.31
05°59′ W	97	24.7	16.1	1.70	—	3.23
22–11–92	145	28.0	24.7	1.89	—	0.20
	194	30.1	29.8	2.20	—	0.32
	387	34.3	57.6	2.33	—	0.42

Intermediate Water (AAIW) and underlying Antarctic Bottom Water (AABW) (Tchernia, 1980).

At the position of the Subtropical Convergence, NADW penetrates into the ACC and contributes to Circumpolar Deep Water (CDW), which, on average, circles several times around the Antarctic Continent forced by the West Wind Drift. At the position where NADW enters the ACC, the relatively warm, salty, oxygen-rich and nutrient-poor NADW tends to divide the CDW into two parts: the Upper Circumpolar Deep Water (UCDW) and the Lower Circumpolar Deep Water (LCDW).

At the southern end of the section the CDW contacts Weddell Sea Deep Water (WSDW), a water mass that obtains its characteristics of low temperature, high oxygen and low nutrient concentrations from deep-water formation in the southern Weddell Sea. Outside the Weddell Sea, the WSDW becomes part of the northward-flowing Weddell Sea Bottom Water (WSBW), eventually forming the Antarctic Bottom Water (AABW). At the research section the American–Antarctic Ridge forms a barrier for the northward transport of AABW, which instead seeks its way over the seafloor more towards the west, near and beyond the Sandwich Islands.

Surface circulation

All surface waters generally drift eastward, forced by the West Wind Drift. At the fronts, the geostrophic velocity is considerably higher than that of the wide stretches of water masses between the fronts. Three fronts were identified at this transect (Veth *et al.*, 1997):

— the Polar Front north of 50°S, meandering with a main frontal jet near 49°S;
— the southern ACC front at the end of the 1.8°C isotherm between 54° and 56°S (Orsi *et al.*, 1995); and
— the ACC–Weddell Gyre Boundary (AWB) at about 58°S.

Table 3. Deep water stations with data on hydrography, nutrients, dissolved and total dissolvable Fe

Station/ position/date	Depth (m)	Salinity	Pot. T (°C)	Oxygen (μM)	NO_3 (μM)	Si (μM)	PO_4 (μM)	Total Fe (nM)	Dissolved Fe (nM)
972	497	34.439	2.265	195.9	35.8	63.9	2.43	—	2.50
48°41′ S	743	34.586	2.204	181.0	34.1	76.9	2.36	—	—
06°00′ W	991	34.693	2.262	191.1	32.1	76.6	2.17	—	0.43
22-11-92	1240	34.753	2.141	204.2	29.7	75.6	2.05	—	2.72
	1486	34.761	1.894	208.0	30.0	80.7	2.05	—	—
Bottom:	1727	34.764	1.686	214.4	29.4	84.7	2.03	—	1.36
4123–4088 m	1973	34.726	1.214	209.8	31.8	102.1	2.14	—	4.11
	2467	34.712	0.827	215.0	32.2	111.1	2.20	—	0.97
	2953	34.682	0.306	216.4	33.1	123.5	2.28	—	1.64
	3105	34.681	0.267	222.8	33.0	124.8	2.24	—	2.80
956	494	34.520	2.058	181.0	36.0	76.4	2.50	—	1.01
50°01′ S	988	34.715	2.023	192.2	32.0	84.7	2.24	—	4.33
05°58′ W	1233	34.746	1.896	—	31.0	85.0	2.16	—	1.04
18-11-92	1479	34.742	1.616	201.9	31.2	91.7	2.16	—	0.63
	1727	34.717	1.159	201.6	32.3	105.3	2.25	—	1.99
Bottom:	1972	34.713	0.953	207.4	32.0	109.6	2.25	—	6.40
2512–2517 m	2219	34.702	0.753	208.9	32.6	115.1	2.30	—	0.98
	2379	34.698	0.633	210.9	32.9	114.9	2.32	—	1.50
	2431	34.696	0.619	211.6	32.7	118.5	2.30	—	0.92
	2460	34.695	0.576	211.6	33.2	120.2	2.31	—	1.93
	2469	34.694	0.576	210.6	32.9	119.5	2.31	—	1.72
951	50	33.927	0.120	353.9	26.7	31.7	1.86	—	—
52°01′ S	101	33.932	−0.210	352.2	26.9	33.1	1.85	0.32	—
06°01′ W	249	34.375	1.381	213.9	35.0	66.8	2.42	1.17	—
17-11-92	495	34.628	1.935	177.4	34.7	86.0	2.38	0.84	—
	741	34.695	1.858	185.0	32.8	89.2	2.26	2.33	—
Bottom:	987	34.728	1.650	196.6	31.7	92.3	2.17	2.01	—
2180 m	1235	34.725	1.371	201.3	32.9	99.3	2.23	2.02	—
	1478	34.710	1.011	202.7	32.4	109.7	2.23	1.95	—
	1726	34.698	0.747	209.2	32.7	115.7	2.27	2.58	—
	1971	34.691	0.547	212.5	32.7	121.1	2.29	6.53	—
	2068	34.687	0.458	214.7	32.8	125.6	2.30	2.67	—
	2117	34.686	0.439	212.3	32.8	126.2	2.31	3.06	—
947	494	34.668	1.710	182.8	33.3	88.9	2.36	1.71	—
53°58′ S	739	34.709	1.538	194.3	32.1	94.3	2.24	1.01	—
06°00′ W	988	34.714	1.324	199.6	31.7	99.1	2.24	2.05	—
15-11-92	1233	34.701	1.025	203.0	32.4	107.9	2.28	—	—
	1481	34.697	0.785	205.0	33.6	112.4	2.30	1.39	—
Bottom:	1724	34.688	0.542	208.6	32.7	120.0	2.33	2.04	—
2627 m	1972	34.682	0.381	214.1	32.8	122.3	2.33	1.61	—
	2120	34.686	0.220	217.4	33.0	127.9	2.34	2.31	—
	2314	34.675	0.172	217.5	33.0	129.6	2.35	—	1.14
	2462	34.672	0.109	218.8	33.2	132.5	2.35	—	0.92
	2522	34.672	0.095	219.4	33.3	132.3	2.36	—	0.69
	2562	34.671	0.079	217.5	33.1	134.9	2.36	—	1.11

(Continued)

Table 3. Continued

Station/ position/date	Depth (m)	Salinity	Pot. T (°C)	Oxygen (μM)	NO_3 (μM)	Si (μM)	PO_4 (μM)	Total Fe (nM)	Dissolved Fe (nM)
911	54	33.868	−1.446	353.3	27.4	43.7	1.92	—	0.62
55°51′ S	96	33.895	−1.501	347.0	27.4	48.4	1.94	—	0.36
06°00′ W	197	34.428	1.313	216.0	34.5	72.7	2.45	—	0.24
03-11-92	292	34.554	1.665	186.2	35.0	82.8	2.43	—	0.90
	391	34.608	1.698	185.0	34.3	86.5	2.42	2.11	—
Bottom:	495	34.654	1.643	187.1	33.8	89.0	2.50	3.83	—
3903–4059 m	792	34.706	1.459	196.2	32.9	96.0	2.25	0.92	—
	988	34.716	1.312	199.9	31.9	99.1	2.27	0.81	—
	1185	34.705	1.036	204.5	31.8	105.6	2.30	8.51	—
	1478	34.690	0.694	208.9	32.5	112.3	2.33	0.46	—
	1777	34.681	0.424	211.5	33.1	116.1	2.35	2.06	—
	1971	34.678	0.324	214.0	32.7	120.0	2.37	2.17	—
	2169	34.676	0.213	215.2	33.0	121.1	2.37	0.66	—
	2361	34.673	0.128	215.8	33.5	123.8	2.36	1.51	—
	2753	34.667	−0.049	225.5	33.3	125.6	2.34	5.56	—
	2949	34.664	−0.127	230.5	32.9	125.9	2.36	4.88	—
	3436	34.659	−0.299	236.8	33.1	133.2	2.38	4.49	—
	3727	34.657	−0.335	237.8	32.9	133.8	2.37	3.10	—
	3833	34.657	−0.343	238.1	33.0	134.6	2.37	2.89	—
	3874	34.657	−0.346	236.9	32.9	135.7	2.36	1.95	—
	3928	34.657	−0.350	241.2	33.1	135.1	2.37	11.89	—
	3969	34.657	−0.349	232.1	32.8	133.6	2.34	16.51	—
866	497	34.689	1.530	193.1	33.1	107.7	2.22	5.04	—
57°41′ S	990	34.696	0.921	206.0	33.1	111.6	2.20	5.62	—
06°22′ W	1482	34.679	0.410	213.3	34.8	122.5	2.27	7.96	—
10-11-92	1973	34.673	0.154	—	33.6	126.9	2.28	2.25	—
	2463	34.665	−0.079	230.8	33.8	130.0	2.31	3.25	—
Bottom:	3194	34.658	−0.312	—	33.5	131.8	2.28	3.58	—
3760–3518 m	3439	34.657	−0.343	—	33.3	130.5	2.27	6.95	—
	3502	34.657	−0.355	235.3	33.1	130.5	2.23	9.67	—
	3675	34.656	−0.375	—	38.3	132.5	2.34	7.92	—
917	59	34.313	−1.820	—	27.3	78.9	2.00	1.79	—
58°28′ S	99	34.328	−1.823	—	27.0	77.1	1.98	0.82	—
05°58′ W	199	34.407	−1.756	—	27.5	76.6	1.98	0.39	—
05-11-92	297	34.631	0.076	—	33.0	111.5	2.36	0.31	—
	396	34.676	0.392	—	34.0	120.2	2.40	1.31	—
Bottom:	498	34.678	0.380	202.1	33.4	120.2	2.40	1.23	—
4946–5028 m	595	34.678	0.328	—	33.5	127.4	2.41	1.41	—
	793	34.676	0.235	—	32.8	128.2	2.35	2.17	—
	987	34.671	0.123	214.5	33.1	125.1	2.37	3.56	—
	1286	34.667	−0.012	—	32.3	127.5	2.33	1.42	—
	1497	34.664	−0.085	222.4	32.6	125.7	2.34	2.27	—
	1773	34.660	−0.216	—	32.2	126.3	2.26	1.63	—
	1972	34.658	−0.282	234.8	33.8	126.6	2.30	0.69	—
	2169	34.657	−0.341	—	32.1	125.4	2.29	2.93	—
	2459	34.654	−0.426	240.4	32.6	124.8	2.28	2.58	—
	2657	34.653	−0.475	—	32.9	124.8	2.38	2.21	—

(*Continued*)

Table 3. Continued

Station/ position/date	Depth (m)	Salinity	Pot. T (°C)	Oxygen (μM)	NO_3 (μM)	Si (μM)	PO_4 (μM)	Total Fe (nM)	Dissolved Fe (nM)
	2950	34.651	−0.527	246.3	32.4	124.6	2.30	3.45	—
	3437	34.649	−0.582	248.4	32.8	123.7	2.31	4.01	—
	3732	34.658	−0.619	251.8	32.8	122.2	2.30	5.29	—
	3925	34.648	−0.640	250.1	32.7	121.2	2.30	3.10	—
	4951	34.644	−0.754	252.4	32.3	117.3	2.28	5.74	—
865	492	34.649	1.751	189.1	(51.1)	88.3	2.37	—	1.10
56°11′ S	988	34.718	1.432	202.6	33.4	95.9	2.29	—	0.99
12°24′ W	1478	34.690	0.730	—	33.8	111.5	2.38	—	0.57
10-09-92	1969	34.681	0.371	218.7	34.6	118.9	2.39	—	—
	2461	34.674	0.118	224.2	36.7	123.3	2.39	—	0.80
Bottom:	2951	34.666	−0.106	232.7	36.1	125.5	2.36	—	—
4887–4885 m	3925	34.654	−0.451	—	33.7	129.7	2.36	—	—
	4509	34.652	−0.516	—	38.1	131.5	2.35	—	—
	4744	34.652	−0.520	250.2	35.4	132.0	2.33	—	1.45
	4828	34.652	−0.523	254.9	42.0	131.9	2.25	—	6.48
979	98	34.125	6.619	—	23.8	8.9	1.65	—	—
45°29′ S	246	34.187	5.065	—	29.8	22.1	2.06	0.54	—
01°08′ E	497	34.187	3.405	—	34.8	55.8	2.41	2.45	—
25-11-92	984	34.421	2.598	—	34.5	65.5	2.41	2.35	—
	1234	34.562	2.520	—	32.3	67.4	2.25	2.18	—
Bottom:	1482	34.677	2.499	—	30.9	68.8	2.15	—	—
4186–4159 m	1728	34.737	2.364	—	29.4	69.6	2.05	2.43	—
	1976	34.774	2.186	—	29.3	70.9	2.01	1.99	—
	2120	34.780	2.074	—	29.4	77.0	2.07	2.01	—
	2317	34.773	1.871	—	29.8	79.9	2.09	1.87	—
	2465	34.769	1.759	—	29.7	82.5	2.09	1.87	—
	2953	34.752	1.403	—	30.7	90.4	2.15	1.98	—
	3198	34.741	1.186	—	31.2	96.0	2.18	—	—
	3198	34.741	1.186	—	31.2	96.0	2.18	2.54	—
	3684	34.713	0.742	—	32.3	109.4	2.28	—	—
	3929	34.706	0.596	—	34.3	110.9	2.29	3.79	—
	4076	34.700	0.522	—	32.9	115.4	2.32	7.54	—
	4076	34.700	0.522	—	32.8	115.7	2.34	5.71	—
	4149	34.698	0.491	—	33.4	116.9	2.34	5.71	—

The Polar Front meanders within a wider range, here called the Polar Frontal region. The site of the Polar Front is associated with the formation of AAIW, which is derived from the combination of Antarctic Surface Water with CDW. It is characterised by a distinct temperature gradient with latitude (Tchernia, 1980). Upon its formation, the subsurface AAIW flows northward into the Atlantic, Indian and Pacific Oceans, while gradually sinking to ~800–1200 m depth and mixing with both deep and surface waters. In our transects only the initial stage of formation of AAIW can be traced between 47 and 48°S in the upper 200 m by a potential temperature between 2.0 and 3.0°C and a salinity minimum of 33.8–33.9. In the *T–S* diagram (Fig. 2) of the most northerly final station 979 (45°29′S,

Table 4. Concentrations of total particulate Al within the first 600 m *of the water column during ANT X/6. Sampling and analyses by F. Dehairs independent of particulate Fe analyses*

Station/transect	Position	Depth (m)	Total particulate Al (nM)
886/5	56°00′ S, 06°00′ W	10	13.5
		50	5.8
		100	2.3
		150	3.1
		200	2.1
		250	2.4
		300	3.5
		350	2.0
		425	3.3
		500	2.2
		600	3.2
891/5	55°01′ S, 06°01′ W	10	6.9
		50	9.3
		100	1.6
		150	2.3
		200	1.8
		250	2.3
		300	2.3
		350	2.5
		425	2.4
		500	1.5
		600	2.1
895/5	53°00′ S, 06°00′ W	10	4.4
		50	3.6
		100	2.0
		150	2.3
		200	1.9
		250	1.6
		300	1.5
		350	1.4
		425	1.6
		500	1.2
		600	0.8
899/5	51°00′ S, 06°00′ W	10	0.0
		50	3.5
		100	2.5
		150	2.2
		200	1.8
		250	1.8
		300	2.0
		350	1.2
		425	1.3
		500	1.7
		600	1.7
903/5	49°00′ S, 06°00′ W	10	16.8
		50	11.6

(*Continued*)

Table 4. Continued

Station/transect	Position	Depth (m)	Total particulate Al (nM)
		100	6.1
		150	3.1
		200	2.7
		250	2.8
		300	2.8
		350	3.7
		425	2.2
		500	1.2
		600	0.9
907/5	47°00′06°00′ W	10	18.5
		50	17.7
		100	8.8
		150	3.6
		200	2.2
		250	2.2
		300	3.1
		350	2.5
		425	2.6
		500	3.1
		600	2.7
939/11	57°30′ S, 06°00′ W	10	10.1
		50	7.8
		100	3.3
		150	2.8
		200	2.6
		250	1.9
		300	1.7
		350	2.1
		425	1.7
		500	1.5
		600	1.3
945/11	55°00′ S, 06°01′ W	10	1.6
		50	2.4
		100	0.7
		150	0.4
		200	0.6
		250	0.5
		300	0.5
		350	0.4
		425	2.1
		500	0.5
		600	0.9
949/11	53°00′ S, 06°01′ W	10	3.3
		50	2.1
		100	0.4
		150	0.5
		200	0.8

(Continued)

Table 4. Continued

Station/transect	Position	Depth (m)	Total particulate Al (nM)
		250	1.0
		300	0.4
		350	0.5
		425	0.5
		500	1.5
		600	0.4
953/11	51°00′ S, 06°00′ W	10	3.7
		50	1.0
		100	0.9
		150	1.1
		200	0.8
		250	0.4
		300	0.8
		350	0.5
		500	0.3
		600	0.4
960/11	49°00′ S, 06°00′ W	10	17.9
		50	9.6
		100	2.8
		150	0.9
		200	0.9
		250	1.4
		300	1.3
		350	0.9
		425	1.2
		500	1.0
		600	1.0
972/12	48°41′ S, 05°59′ W	10	10.2
		50	5.7
		100	1.4
		150	1.6
		200	1.7
		250	1.7
		300	1.7
		350	0.8
		425	1.5
		500	3.1
		600	1.1

01°08′E), the core of the AAIW between 500 and 1000 m is indicated by the salinity minimum of 34.2–34.4 at a potential temperature of between 2.5 and 3.5°C. The Polar Front shows the strong velocity shear, meandering and interleaving as is commonly associated with energetic frontal regions (Veth *et al.*, 1997). South of the Polar Front a mixed layer of Antarctic Surface Water (AASW) occurs in the upper 300 m, with salinities between 33.2 and 34.4 and potential temperatures between −1.5 and −0.5°C. Still, there is a remainder of Winter Water identifiable between 150 and 250 m, unaffected by seasonal warming. At

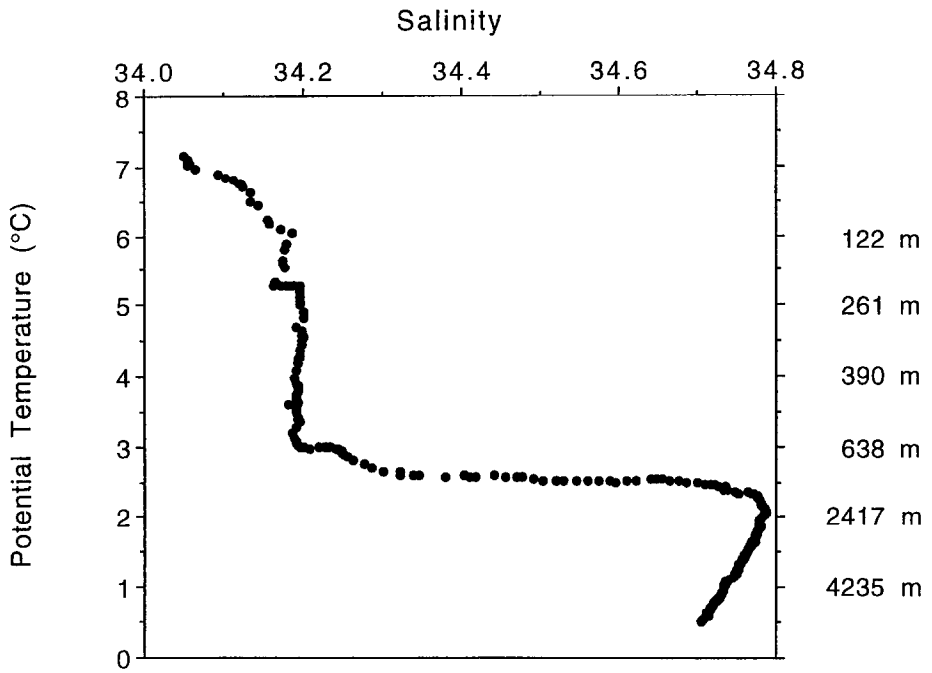

Fig. 2. *T–S* diagram of station 979 at 45°29'S, 01°08'E.

station 979, north of the Polar Front, SubAntarctic Surface Water (SASW) has a potential temperature between 4° and 7°C and a salinity between 34.1 and 34.4.

DISTRIBUTION OF IRON IN SURFACE WATERS

Dissolved Fe in Antarctic surface waters south of the Polar Frontal region

The AASW south of the Polar Front can be considered to be representative of the vast Antarctic Ocean, particularly with respect to its low biological productivity. Dissolved Fe concentrations were on average as low as 0.48 nM (transect 5, Fig. 3a) and 0.31 nM (transect 11, Fig. 3b) at a depth of 40–300 m. The minimum for dissolved Fe was 0.17 nM at 51°S. During section 11 somewhat higher dissolved Fe at ~1 nM was encountered at 54°S, perhaps due to some input from previous melt. Dissolved Fe concentrations increased with depth, and, at a depth of 200–400 m, reached values consistent with ACC dissolved deep-water concentrations ranging from 0.6 to 1.1 nM. Further westward, in offshore Drake Passage waters, Martin *et al.* (1990a) reported dissolved Fe concentrations ranging from 0.10 nM to 0.26 nM for the surface waters (30–300 m), and 0.40–0.76 nM at 550–1450 m intermediate depths when disregarding rejected values from 0.52 to 1.55 nM.

Total dissolvable Fe in surface waters outside of the frontal regions

The concentrations of total dissolvable Fe within the first 10 m depth are about 2.0 nM south of the Polar Frontal region at transect 5 (at 52° and 53°S) (Fig. 4a) and are similar at

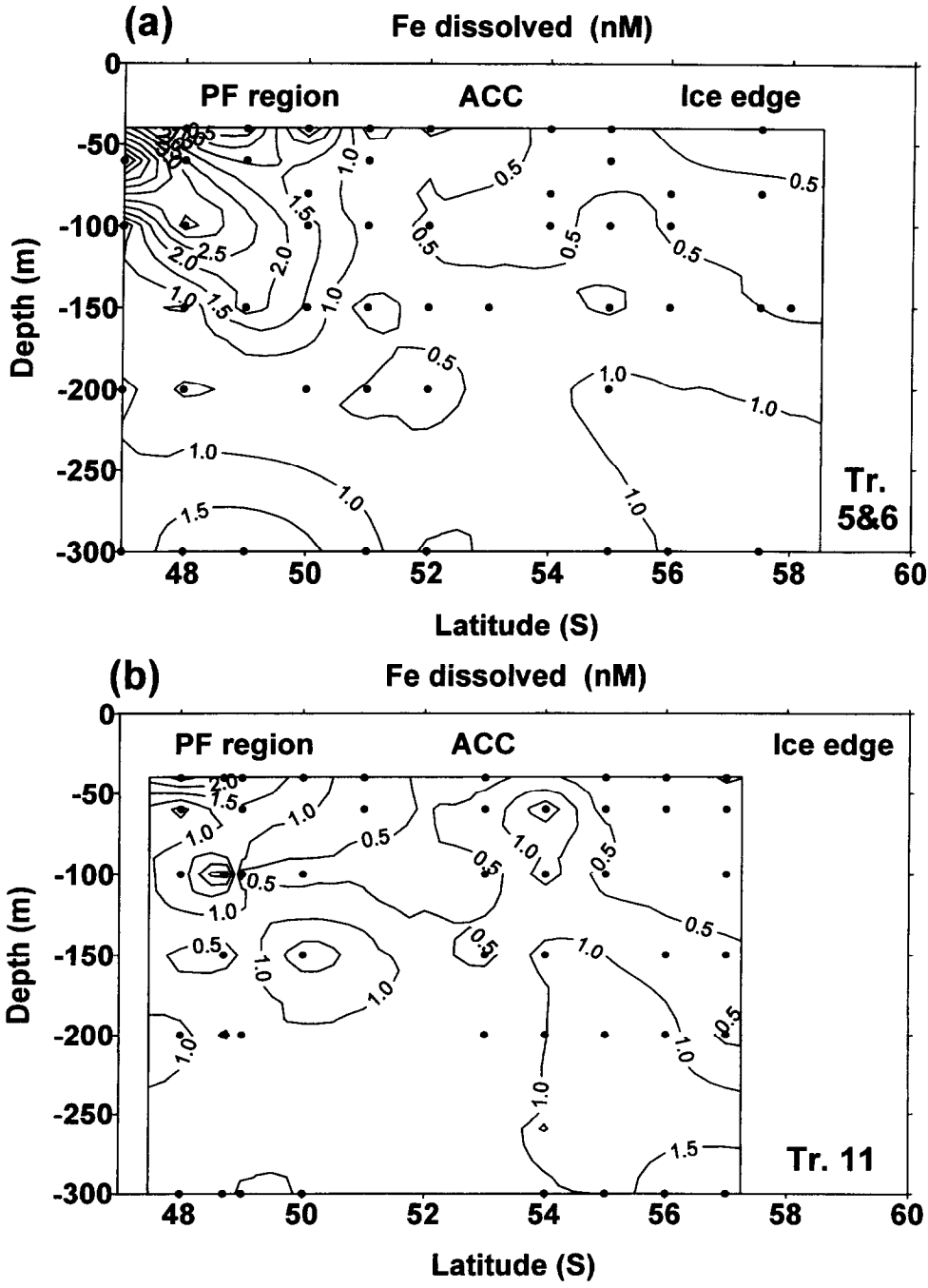

Fig. 3. Section plot of dissolved Fe in the upper water column along the 6°W meridian: (a) at combined transect 5 and 6; (b) at transect 11.

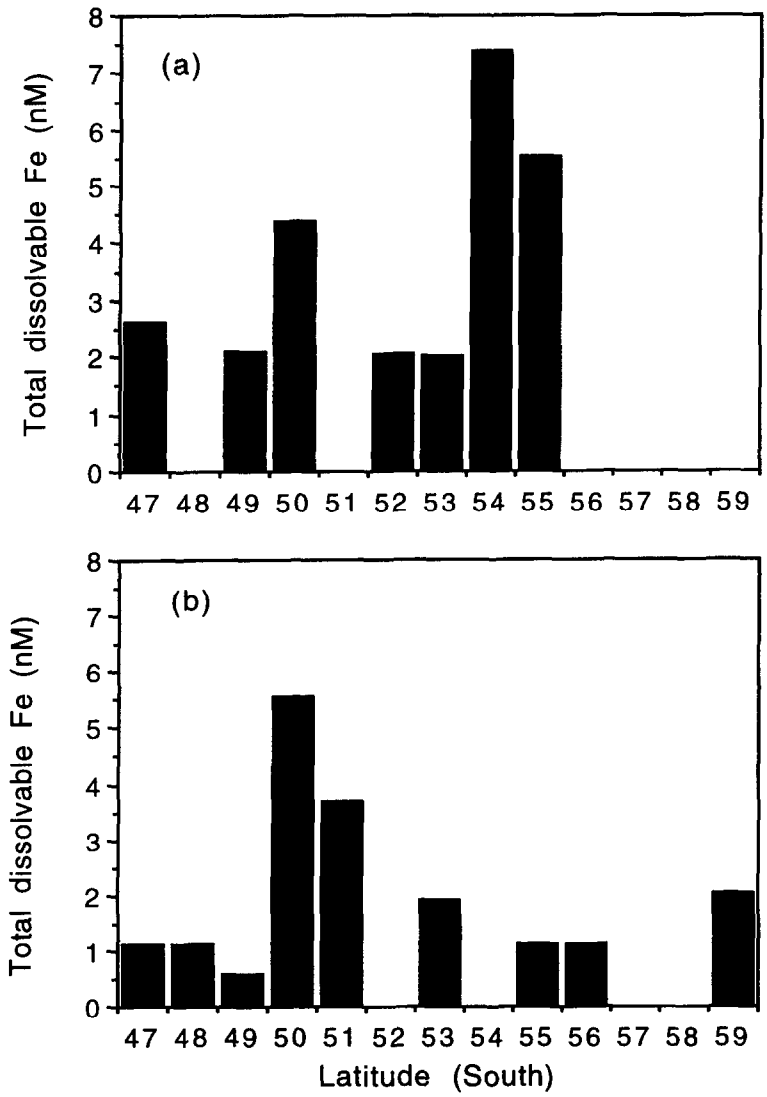

Fig. 4. Total dissolvable Fe within the first 10 m of the water column: (a) at transect 5; (b) at transect 11.

transect 11 (53°S) (Fig. 4b). North of the Polar Frontal region the total dissolvable Fe concentration at transect 5 reaches 2.6 nM (at 47°S), whereas along transect 11 values range between 0.6 and 1.1 nM (at 47°, 48° and 49°S).

Dissolved Fe in surface waters of the Polar Frontal region

In the more rapidly eastward-flowing Polar Frontal region, the average concentration of dissolved Fe is 1.87 nM (transect 5, Fig. 3a), then decreasing as spring develops to an

average of 1.14 nM (transect 11, Fig. 3b). The latter decrease is consistent with significant uptake and removal of Fe from seawater, this being supported by a depletion of ^{234}Th in transect 11 (Rutgers van der Loeff *et al.*, 1997). The section plot of dissolved Fe along the 6°W meridian, at combined transects 5 and 6, shows the pronounced Fe maximum at 48–50°S in the upper 150 m. This can be ascribed to shelf sources. Similarly, in the more enclosed Weddell Sea, Westerlund and Öhman (1991) reported values ranging from 0.24 to 5.59 nM, whereas Nolting *et al.* (1991) found about 1.5–4 nM in the Scotia Sea, which apparently was influenced by the Weddell Sea at the front of the Weddell–Scotia Confluence. For waters in Gerlache Strait, near the Antarctic Peninsula, higher concentrations at about 7 nM have been found (Martin *et al.*, 1990a). At the extensive shelf around the Signy Island the dissolved Fe just after the sea-ice retreat was as high as ~50 nM at a shallow station, very similar to concentrations in inshore waters of, for example, the North Sea.

Total dissolvable Fe in surface waters in the frontal regions

Within the three fronts passed during this cruise, the total dissolvable Fe concentrations are higher than in the rest of the surface ACC waters. In the Polar Frontal region the total dissolvable Fe reaches a concentration of 4.4 nM and 5.6 nM for transect 5 at 50°S (Fig. 4a) and 11 at 50°S (Fig. 4b), respectively. In the southern ACC front it reaches 7.4 nM at transect 5. Input within the Marginal Ice Zone (MIZ) resulting from sea-ice melting was observed during transect 11 at 59°S, with a total dissolvable Fe concentration of 2.0 nM.

DISTRIBUTION OF IRON IN DEEP WATERS

Dissolved Fe in deep waters

In the southern branch of the ACC (51–56°S), the Circumpolar Deep Water (upper and lower) shows dissolved Fe ranging from 0.6 to 1.1 nM at one station (56°11′S, 12°24′W), and 0.7–1.1 nM at another station (53°58′S, 06°00′W) (Table 5). This is similar to dissolved deep concentrations of Fe in the deep equatorial Pacific Ocean (mean at ~0.5–1.5 nM for a range of 0.44–2.6 nM; Landing and Bruland, 1987), the deep northwest Indian Ocean (~1–2 nM; Saager *et al.*, 1989), the North Atlantic Ocean south of Iceland (0.3–0.64 nM, Martin *et al.*, 1993), the northwest Atlantic (0.4–0.8 nM, Wu and Luther, 1994), and the deep northeast Pacific (0.6–0.7 nM, Martin *et al.*, 1989) (Table 6). In the Polar Frontal region the deep Fe concentrations, especially at the station at 48°41′S near the jet of the Polar Front, do reach higher values (0.4–2.8 nM) presumably due to Fe input from shelf sources as discussed below.

Total dissolvable Fe in Antarctic deep waters

Total dissolvable Fe concentrations (unfiltered) in the UCDW decrease south from the Polar Front, a decrease from 2.0–2.3 nM at 52°01′S to 1.0–1.7 nM at 53°58′S to 0.9 nM at 55°51′S (Table 5). This may be simply a dilution effect as a result of mixing of Polar Front waters with adjacent water masses of lower total Fe contents; yet some removal by settling of particles likely also takes place. Total dissolvable Fe concentrations in the LCDW are

Table 5. Average deep concentrations of dissolved Fe and total dissolvable Fe

Research area	Dissolved Fe (nM)	Total dissolvable Fe (nM)
48°41′ S	0.4–2.7 (UCDW)	
06°00′ W	1.0–2.8 (LCDW)	
Jet of the Polar Front		
50°00′ S	0.6–1.0 (UCDW)	
05°58′ W	1.0–2.0 (LCDW)	
Polar Frontal region		
52°00′ S		2.0–2.3 (UCDW)
06°01′ W		2.0–3.1 (LCDW)
53°58′ S		1.0–1.7 (UCDW)
06°00′ W	0.7–1.1 (LCDW)	1.4–2.0 (LCDW)
55°51′ S		0.9 (UCDW)
06°00′ W		0.5–2.2 (LCDW)
		2.0–16.5 (AABW)
57°41′ S		2.2–8.0 (LCDW)
06°22′ W		3.2–9.7 (AABW)
56°11′ S	1.0–1.1 (UCDW)	
12°24′ W	0.6–0.8 (LCDW)	
	1.5–6.5 (AABW)	
45°29′ S		2.4 (AAIW)
01°08′ E		1.3–2.4 (UCDW)
		2.0–7.5 (LCDW)

always higher than in the UCDW. This is consistent with input at the nepheloid layer and conceivable ridge crest sources as discussed below. Total dissolved Fe concentrations in the AABW (3.2–9.7 nM) are higher than those of the other water masses in the ACC. This is also apparent from total dissolvable Fe concentrations (Table 5). The high Fe in AABW likely is due to input from the nepheloid layer and Fe input from the shelf during formation of AABW. Westerlund and Öhman (1991) reported total dissolvable Fe concentrations between 1 and 25 nM at the Weddell Sea shelves, which are the ultimate sites of AABW formation. They demonstrated transport of Fe from the shelves into the Weddell Sea basin, where shelf water contributes to the formation of WSDW, which forms an important contribution to the formation of AABW. Nolting *et al.* (1991) reported dissolved Fe concentrations from 3.2 to 4.2 nM for UCDW, from 1.6 to 5.7 nM for LCDW, and from 1.8 to 4.0 nM for AABW for a deep station at 57°00′S, 48°24′W in the Scotia Sea.

Total dissolvable Fe in subAntarctic deep waters

One station was sampled in the subAntarctic Ocean at 45°29′S, 01°08′E, near the margin of the Cape Basin (Fig. 5). Here the AAIW had a total dissolvable Fe concentration of about 2.4 nM. Within the UCDW the total dissolvable Fe concentration decreased to about 2.0 nM, but increased again within the nepheloid layer of the LCDW to concentrations as high as 7.5 nM near the seafloor. The total Fe maximum in the AAIW can be attributed to

Table 6. Calculations of the annual upward transport of dissolved Fe into surface waters of the ACC and the Gulf of Alaska (Station "Papa"). Also listed are the aerosol input estimates, here assuming 10% dissolution of the total aeolian input.

$$N^2 = (-g/\rho)(\delta\rho/\delta z) \quad (1)$$

$$J_a = w[\mathrm{Fe}] \quad (2)$$

$$J_d = K_z(\partial[\mathrm{Fe}]/\partial z) \quad (3)$$

	ACC station 865	Northeast Pacific Station "Papa"
w	15×10^{-5} cm s^{-1} (Gordon *et al.*, 1977)	5×10^{-5} cm s^{-1} (Miller *et al.*, 1991a,b)
(max. w)	30×10^{-5} cm s^{-1} (Gargett, 1991)	10×10^{-5} cm s^{-1} (Martin *et al.*, 1989)
Deep [Fe]	1×10^{-6} mol m^{-3}	0.6×10^{-6} mol m^{-3} (Martin *et al.*, 1989)
J_a	**1.5×10^{-12} mol m^{-2} s^{-1}**	**0.3×10^{-12} mol m^{-2} s^{-1}**
N^2	3.4×10^{-5} (radians s^{-1})^2 (140–250 m depth)	1.6×10^{-4} (radians s^{-1})^2 (20–50 m depth)
K_z	0.3×10^{-4} m^2 s^{-1} 140–250 m depth)	0.5×10^{-5} m^2 s^{-1} (20–50 m depth)
∂[Fe]/∂z	6.1×10^{-9} mol m^{-4} (140–250 m depth)	2.8×10^{-10} mol m^{-4} (20–50 m depth)
J_d	**0.18×10^{-12} mol m^{-2} s^{-1}**	**0.14×10^{-14} mol m^{-2} s^{-1}**
$J_t = J_a + J_d$	**1.7×10^{-12} mol m^{-2} s^{-1}**	**0.31×10^{-12} mol m^{-2} s^{-1}**
Annual Fe aerosol flux	3 mg m^{-2} year^{-1} (Duce and Tindale, 1991)	30 mg m^{-2} year^{-1} (Duce and Tindale, 1991)
"Dissolved" Fe aerosol flux	**0.17×10^{-12} mol m^{-2} s^{-1}**	**1.7×10^{-12} mol m^{-2} s^{-1}** $0.9–1.9 \times 10^{-12}$ mol m^{-2} s^{-1} (Duce, 1986)
N	Brunt–Väisälä frequency	(radians s^{-1})
g	Gravity	$g = 9.81$ m s^{-2}
ρ	Density	(kg m^{-3})
z	Negative depth	(m)
[Fe]	Concentration dissolved Fe	(mol m^{-3})
w	Vertical velocity	(cm s^{-1})
K_z	Vertical turbulent diffusivity	(m^2 s^{-1})
J_a	Advective flux	(mol m^{-2} s^{-1})
J_d	Eddy-diffusive flux	(mol m^{-2} s^{-1})
J_t	Total upward flux	(mol m^{-2} s^{-1})

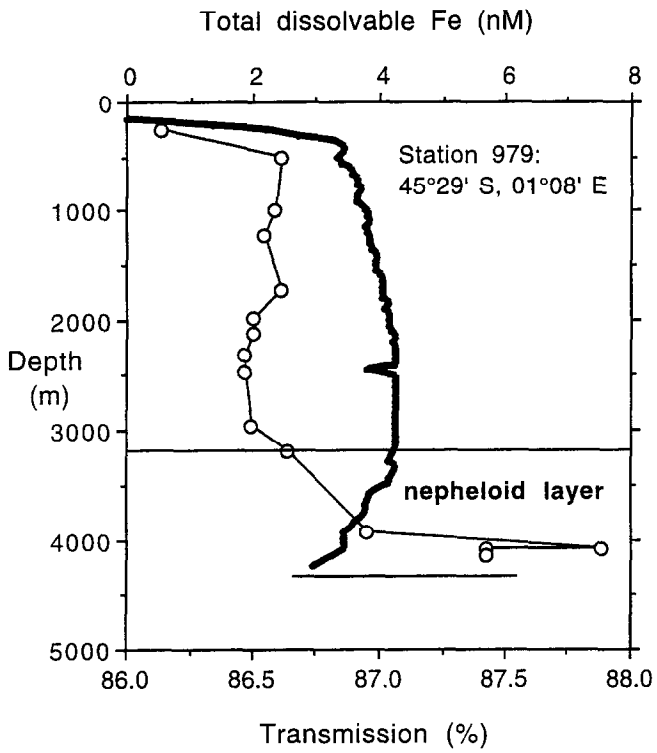

Fig. 5. Vertical profile at 45°29'S, 01°08'E of total dissolvable Fe in SASW (0–500 m), AAIW (500–1000 m), UCDW and LCDW compared with data from the transmissometer.

Fe associated with particles originating from AASW, which mixes with CDW to form AAIW. Symes and Kester (1985) found the same general shape for the depth profile of total Fe in the northwest Atlantic Ocean. They observed a higher percentage of particulate Fe, compared with dissolved Fe, within the upper 500 m, as well as from 1500 m to the bottom (3000 m). These higher percentages of total Fe are associated with particulate matter in surface waters, where particles tend to accumulate in the pycnoclines, and near the bottom nepheloid layer, where they are resuspended from bottom sediments (Symes and Kester, 1985). An increase in the total dissolvable Fe concentration due to the existence of a nepheloid layer (as observed from the decrease of the light transmission) also was found at Antarctic proper stations 866, 917, 911 and 951 (Fig. 6a–d).

SOURCES OF IRON IN SURFACE WATERS

The supply of iron to surface waters is of critical importance for biological productivity (Gran, 1931; de Baar, 1994). In Antarctic surface waters, the concentrations of both the major nutrients and dissolved Fe are only somewhat lower than those found in the underlying deep waters. For the major nutrients, the supply from below, by the intense wind-driven upwelling, apparently exceeds the rate of incorporation in biota and subsequent removal from surface waters. Similarly, the supply of dissolved Fe may be from below by upwelling and vertical mixing, but other sources are conceivable. Briefly,

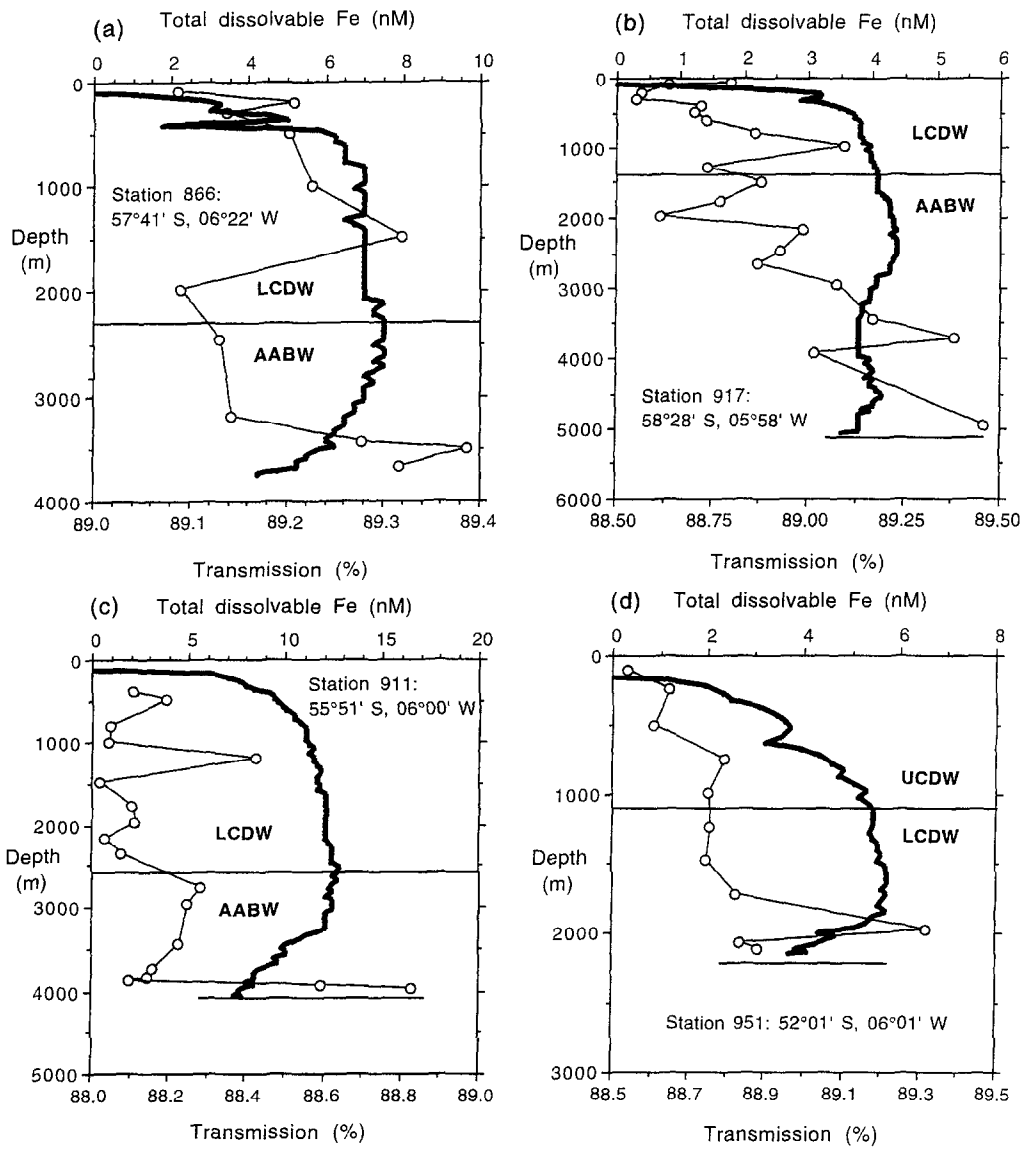

Fig. 6. Vertical profiles at four stations of total dissolvable Fe compared with data from the transmissometer. (a) Station 866: 57°41'S; 06°22'W. (b) Station 917: 58°28'S; 05°58'W. (c) Station 911: 55°51'S; 06°00'W. (d) Station 951: 52°01'S; 06°01'W.

four different inputs of iron to surface waters can be defined: (i) vertical input from below by upwelling and eddy diffusion; (ii) atmospheric input of continental dust, including input of accumulated dust upon spring melting of sea-ice; (iii) input from melting icebergs; and (iv) lateral input from sediments at continental margins. The relative importance of each source term for regions and fronts of the Antarctic Ocean can be compared with their significance for the other HNLC zones. Here the Southern Ocean will be compared with the subArctic Pacific Ocean.

Vertical input from below by upwelling and mixing

Vigorous wind-driven upwelling and eddy diffusion, in combination with somewhat higher deep water concentrations of 0.6–1.1 nM (southern ACC zone), are responsible for a larger upward supply of dissolved Fe from deep to surface waters in the ACC than in the subArctic Pacific region of the Gulf of Alaska. The wind stress in the ACC region is about twice as high as that in the northern North Pacific (Trenberth *et al.*, 1990), with a seasonality where during austral winter the wind stress is on average about twice that in summer. For the ACC, the consistently high wind velocities, the little variation in wind direction, the absence of land barriers, and the slightly higher deep water concentrations of dissolved Fe make Ekman pumping about four times stronger than in the North Pacific Ocean (Table 6).

In Antarctic waters, the density stratification is about five times weaker than in the Gulf of Alaska, as indicated by the density gradient at the pycnocline between the wind-mixed surface layer and deep water (Fig. 7). Station 865, for example, has a density stratification of about 3.4×10^{-3} kg m^{-4} in the surface boundary layer between 140 and 250 m. At station "Papa" the density stratification between 20 and 50 m is about 1.5×10^{-2} kg m^{-4} (August 1987) (Martin *et al.*, 1989). In May 1988, the density stratification pycnocline at station "Papa" between 120 and 130 m (Miller *et al.*, 1991a,b) was about 3.7×10^{-2} kg m^{-4}, which is in the same order as in August. An average value of 2.6×10^{-2} kg m^{-4} is used for further calculations on the Gulf of Alaska station.

Different methods of determination, and different depth ranges, yield different values for the eddy diffusion coefficients, K_z. For our calculation, the linear relationship of Broecker (1981) between K_z and N^2, the square of the Brunt–Väisälä frequency, is used. This linear relationship is consistent with measurements done by Ledwell *et al.* (1993), whose K_z nicely

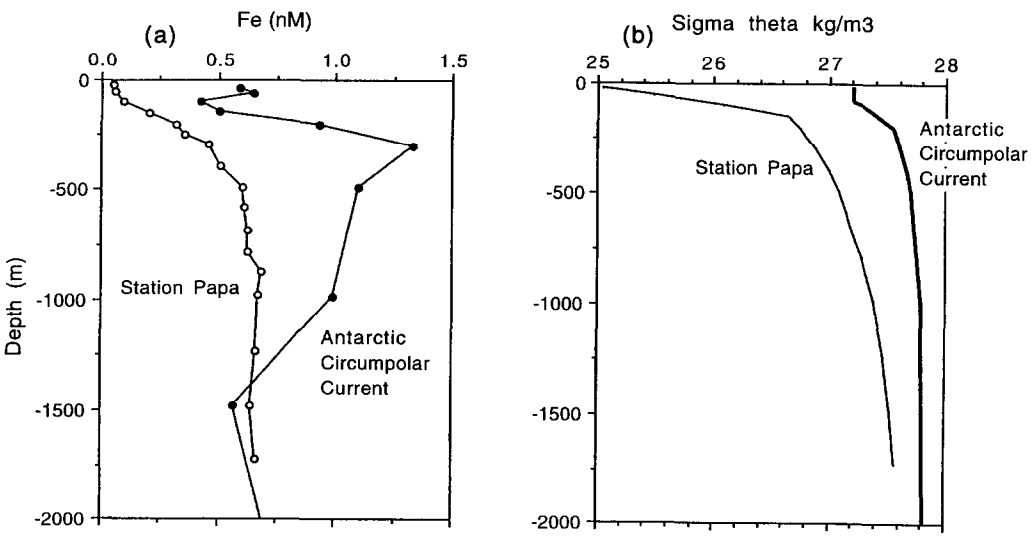

Fig. 7. (a) Filtered Fe (nM) in the upper 2000 m water column at 56°S, 12°W in the southern branch of the ACC (these data) and at Station "Papa" (50°N, 145°W, Martin *et al.*, 1989) in the sub-Arctic Pacific, Gulf of Alaska. Both datasets were used for the calculation of Fe input into the surface waters by upward transport (Table 6). (b) Potential density in the upper 2000 m water column at 56°S, 12°W in the ACC (these data) and at 50°N, 145°W at station "Papa" (Martin *et al.*, 1989).

fits into the density stratification data of Geosecs. The K_z values determined in this way are about 3×10^{-5} m^2 s^{-1} and 0.5×10^{-5} m^2 s^{-1} around Antarctica and in the northeast Pacific Ocean, respectively. This is about 6-fold higher around Antarctica than in the Pacific. Garcon *et al.* (1992) calculated a K_z of 0.8×10^{-5} m^2 s^{-1} in the sub-surface layer at station Papa, quite consistent with the K_z calculated from the Broecker method. Moum and Osborn (1986) have shown that the diapycnal eddy diffusivity does not exceed 10^{-5} m^2 s^{-1} in the upper 400 m in the western North Pacific.

Overall the total upward flux J_t (largely due to Ekman pumping with some extra by eddy diffusion) of dissolved Fe is estimated to be in the order of 1.68×10^{-12} mol m^{-2} s^{-1} in the ACC, about five times larger than the 0.31×10^{-12} mol m^{-2} s^{-1} in the subArctic Pacific Ocean (Table 6). Finally, density gradients in the Polar Frontal region are less than in the southern ACC zone (Veth *et al.*, 1997). Thus, upward transport of Fe by eddy diffusion in the Polar Frontal region may be somewhat more intense than in the overall ACC zone, conceivably leading to modestly higher values for overall upward transport in the Polar Frontal region.

The cellular Fe requirements of phytoplankton are not well known. Sunda *et al.* (1991) reported a ratio of (Fe:C) = $\sim 2 \times 10^{-6}$ for an oceanic diatom. For prokaryotic cyanobacteria, ratios of (Fe:C) > 2×10^{-5} have been found (Brand, 1991). Assuming an average elemental ratio Fe/C of about 10^{-5} for phytoplankton, the supply from below would sustain a daily primary production of about 170 mg C m^{-2} day^{-1} or twice that value, i.e. 340 mg C m^{-2} day^{-1}, when assuming an *f*-ratio of 0.5 for recycling of Fe within the plankton community. These values compare well with the 80–300 mg C m^{-2} day^{-1} actually observed for primary production in the southern ACC surface waters (Jochem *et al.*, 1995). The corresponding potential for primary production on the basis of upwelled nitrate (at typical measured *f*-ratio ~ 0.5 (Goeyens, personal communication 1996)) is much higher, ~ 720 mg C m^{-2} day^{-1}. This demonstrates that only part of the nitrate supply is utilized, i.e. the Antarctic Paradox which now appears, at least partly, explained by insufficient supply of Fe. These calculations had been briefly reported previously (de Baar *et al.*, 1995).

More recently, for the equatorial Pacific Ocean the same calculation has been applied, yielding an upward supply of $\sim 1.4 \times 10^{-12}$ mol m^{-2} s^{-1} of dissolved Fe, similar to the value for the Antarctic Ocean. Yet for the equatorial Pacific itself this would correspond to only about 20% of the potential productivity on the basis of upwelled nitrate (Coale *et al.*, 1996).

Our calculations are based on annual mean transport coefficients. In reality, the lower wind velocity during austral summer (Trenberth *et al.*, 1990) would lead to a lower value for the upward supply of Fe, where on the other hand the Wind Mixed Layer would stabilize at a shallower depth. This, together with better summer insolation, provides a more favourable light climate for bloom development. The opposing seasonality of Fe supply and light gives rise to optimal conditions for phytoplankton growth in late spring or early summer, when at least some Fe is still available from supply in winter and early spring, and light conditions have become more favourable for growth. This scenario is not inconsistent with the general decrease of dissolved Fe in the southern ACC from 0.49 nM at section 5/6 (24 October–6 November 1992) to 0.31 nM at section 11 (10–21 November 1992), whereas recent observations later in the season (and also more easterly away from land sources at 6–12°E) tend to be lower again, about 0.2 nM (January 1996, de Jong and de Baar, unpublished results).

Atmospheric input of continental dust

The Southern Ocean is known to receive the lowest atmospheric dust loads in the world (Prospero, 1981) and, consequently, the lowest atmospheric Fe input. South of the equator, the concentration of dust in the atmosphere is about five to six times lower than in the northern hemisphere due to the lower abundance of continents. On average Fe constitutes about 3.5% of the of mineral matter (Taylor and McLennan, 1985).

The transportation and deposition of mineral aerosol are highly variable due to the episodic nature of dust generation, transport and deposition. The available flux calculations of total Fe are based on measurements of atmospheric dust at a small number of locations over the globe, in combination with a deposition model. On this basis, Duce and Tindale (1991) provided a best estimate of the flux of total Fe from the atmosphere into the surface oceans. From their Fig. 8 the total Fe deposition in the region of the 6°W meridian transect was taken to be about 3 mg m^{-2} $year^{-1}$, by rough interpolation. Between 10 and 50% of the total atmospheric Fe deposition enters the sea as dissolved Fe (Duce and Tindale, 1991). A considerable portion of Fe in marine aerosols has the Fe(II) valency due to photochemical reactions during atmospheric transport (Duce and Tindale, 1991; Zhuang *et al.*, 1992). This Fe (II) is readily soluble, and about half of total Fe deposition may well become available in seawater and taken up by phytoplankton. Here assuming that 10% of the total Fe flux will become dissolved Fe, some 0.17×10^{-12} mol m^{-2} s^{-1} of dissolved Fe is added from aerosols into the Polar Front region of the 6°W meridian transect. The same considerations for the north Pacific site yield 1.8×10^{-12} mol m^{-2} s^{-1} for input of "dissolved Fe", i.e. similar to the Antarctic upwelling supply (see above) but ten times higher than the aerosol supply at the Polar Frontal region of the Southern Ocean. Hence it appears that the surface waters of the open Antarctic Ocean and the subArctic Pacific Ocean have similar amounts of Fe supply, coming from below and above. Similarly, for the equatorial Pacific, the Fe also has been suggested to be supplied from below, rather than above (Coale *et al.*, 1996).

Caveats here are the fact that the total Fe deposition is only a best estimate, and the uncertainty of the assumed 10% rather than say 50% of total aeolian Fe being allowed to dissolve. Also all the above estimates are annual means, while at least Antarctic upwelling likely varies seasonally with wind forcing, and aeolian input definitely is episodic or at least seasonal. A lower abundance of crustal aerosol in the Antarctic continental atmosphere was found during the winter months than during austral summer (Cunningham and Zoller, 1981; Wagenbach *et al.*, 1988). This has been explained by greater snow cover and moisture of southern hemisphere continents as the ultimate source regions (Dick, 1991), i.e. South America as the source region of our study site.

Recently Kumar *et al.* (1995), for a suite of sediment cores in the same general Atlantic research region and using assessments of sedimentation rate on basis of modelling accumulation of radioisotopes, arrived at rates of local sedimentation of total Fe in the modern Holocene era. These Fe input rates ranged from ~ 50 mg m^{-2} $year^{-1}$ ($= 5$ mg cm^{-2} $kyear^{-1}$; Kumar *et al.*, 1995, their figs 3d and 4e) at a site north of the Polar Front, to a rather uniform 30 mg m^{-2} $year^{-1}$ at three sites south of the Polar Front to 49–54°S. Firstly, these total deposition rates are about an order of magnitude higher then the best estimates of Duce and Tindale (1991). Secondly, the higher deposition rate in the subAntarctic or Polar Frontal Zone just north of the actual Polar Front jet was ascribed to aeolian supply of dust from the Patagonian desert. Such, likely very episodic, dust input also may be the cause of the maxima of dissolved Fe and particulate Fe and Al here reported at

the Polar Frontal region (meandering between ~48–50°S) and beyond at 47°S. On the other hand the strong coincidence of these maxima with Polar Front hydrography would render an internal oceanic source term more likely, i.e. the shelf and slope sediments of continental margins as discussed below.

Towards the south in the open ACC and the seasonally ice-covered ACC and Weddell Gyre the aeolian input would be low, here assumed to be at about 1 mg m^{-2} $year^{-1}$ (Duce and Tindale, 1991). Aerosol deposition accumulates over the winter in sea-ice and snow. Again only 10–50% of such flux would be deemed dissolvable. At three stations, ice samples were taken from ice-floes having a thickness of ~80–120 cm. Here we take a concentration of ~30 nM as a typical value for total dissolvable Fe in sea-ice and snow (Table 7). For a 1 m-thick sea-ice cover this would correspond to a deposition rate of 30 μmol m^{-2} $year^{-1}$ or 1.7 mg m^{-2} $year^{-1}$. This appears in keeping with the 1 mg m^{-2} $year^{-1}$ of Duce and Tindale (1991). However the sea-ice cover exists for only part of the year, say 6–9 months. Also in those months of austral winter the aeolian input is likely lower than in late spring and summer. For both reasons the value of 1.7 mg m^{-2} $year^{-1}$ is deemed to be a low estimate as compared to a high estimate of ~30 mg m^{-2} $year^{-1}$ of Kumar *et al.* (1995). Nevertheless, the 30 nM in ~1 m thick sea-ice would, upon spring melting of the ice and vertical mixing over a 75 m deep Wind Mixed Layer, give rise to an increase in the dissolved Fe in the Marginal Ice Zone of 0.4 nM. This is comparable to the increase of ~0.5 nM at 54°W in transect 11 relative to preceding transect 5/6 (Fig. 3). However when taking into account that only 10–50% of total dissolvable Fe in sea-ice would in fact dissolve in seawater, the input of dissolved Fe would be less than 0.4 nM.

In summary, the aeolian input of total Fe to the Antarctic Ocean is very low, but uncertainties within an order of magnitude do exist for both the total input and the dissolvable fraction available for phytoplankton.

Icebergs and ice-rafting debris

At the Weddell–Scotia Confluence (46–50°W), studied during the 1988 EPOS programme, large, visibly dirty, icebergs were observed (de Baar *et al.*, 1990). The majority would be derived from the Filchner ice shelf and carried along with the rotating conveyor belt of perennial pack-ice cover of the western Weddell Sea (Eicken, 1992). This sea-ice, due to its ~2 years' age and close proximity to South American aerosol source regions, also would have accumulated relatively more dust than at the 6°W meridian. Overall the MIZ at the Confluence receives a steady supply of relatively Fe-rich icebergs and sea-ice, which, upon melting, would favour plankton growth also due to meltwater stabilization. Otherwise the Confluence is downstream from the Peninsula, and would also

Table 7. Sea ice- and snow- Fe data from ice-floes with a thickness of 80 cm

Type of ice	Station 866 57°45′ S, 06°29′ W	Station 919 59°30′ S, 06°00′ W	Station 930 59°30′ S, 06°00′ W
Surface snow	52.6 nM	31.3 nM	
Ice-core	26.3 nM	10.8 nM	
Brine	64.6 nM	19.8 nM	
Brown ice (algae)			99.3 nM

receive Fe from sediment sources at the extensive shelves in that region. Continental input, whether from icebergs, aerosols or margin sediments, was also indicated by a high particulate Al maximum of 30 nM at ~200 m depth in the Confluence region of a section at 49°W (Dehairs *et al.*, 1992).

At the MIZ of the ANT X/6 sections at 6°W some 50–60 icebergs were commonly observed within a 22-km wide observational range, the icebergs surprisingly tracking the retreat of the ice-edge with ongoing season (van Franeker, 1994). In the Polar Frontal region a smaller but consistent accumulation of the order of two to ten bergs per 22 km width range was observed. Compared to other cruises and years, the high abundance of icebergs in the Polar Frontal region was rather anomalous. Within the Polar Frontal region the ambient seawater is at ~0.5°C as compared to as low as −1.5°C in the southern ACC and Weddell Gyre. Hence significant melting may take place in the Polar Frontal region, and may, at least partly, contribute to the general drop of salinity at the Polar Frontal region (Veth *et al.*, 1997). Such melting of icebergs would contribute some Fe. The Fe content in glacial ice from an iceberg at 48°S and 6°W (station 964) in the Polar Frontal region was 20.4 nM. Surface water samples from the direct vicinity of this iceberg varied from 1 to 9 nM Fe, hinting at some local influence immediately around the melting berg. For the whole region of the Polar Front the maximum Fe input of icebergs may be assessed from the local salinity minimum. Because the Polar Front is the formation area of AAIW and the boundary between subAntarctic Surface Water and AASW, the original salinity of water in the Polar Frontal region without the influence of meltwater cannot be determined. Assuming a salinity of 33.9 as observed north of the Polar Frontal region and a decrease in salinity of 0.05 within the Polar Frontal region, 1 m^3 seawater would contain about 1.5 l "meltwater". Assuming 10–100 nM Fe in water from melting icebergs, as analysed for samples during this cruise (Table 7), 0.015–0.15 nmol Fe was added to 1 l seawater. This is not enough to explain an average input of 1–1.5 nM, which therefore must be attributed mainly to other sources such as the shelf input discussed below.

The supply of Fe from continental margins into the Polar Frontal region

The position of the Fe maxima in the Polar Frontal region coincides with the largest calculated geostrophic velocity of about 25 cm s^{-1} (Veth *et al.*, 1997). Along the southern ACC part of the section, the geostrophic velocity varies from 5 to 10 cm s^{-1}. We propose that the high Fe concentrations within the rapidly eastward flowing Polar Frontal jet may well have originated from Fe input of the shelf from the South American continent. Similarly, in the Antarctic Peninsula region, Martin *et al.* (1990a), Westerlund and Öhman (1991) and Nolting *et al.* (1991) reported a diagenetic input from shelf sediments in the neritic Gerlache Strait, in the Weddell Sea, and over the shallow South Orkney shelf.

The Polar Front traverses the Drake Passage in deep waters (Peterson and Stramma, 1991; their fig. 21). However, it then flows north-eastward across the Scotia Ridge, meandering in the zone between the Falkland Plateau and South Georgia, and then further in a north-easterly direction towards the ~50°S region (Peterson and Stramma, 1991; their fig. 22). Within the overall energetic Antarctic Ocean, the Polar Front stands out as the most dynamic feature (Fig. 8), capable of energetic interaction with the benthic boundary layer of South American shelf and slope sediments. Moreover, baroclinic eddies, which occur in narrow regions where frontal jets change their course (Veth *et al.*, 1997), may well serve as a vertical transport component for Fe.

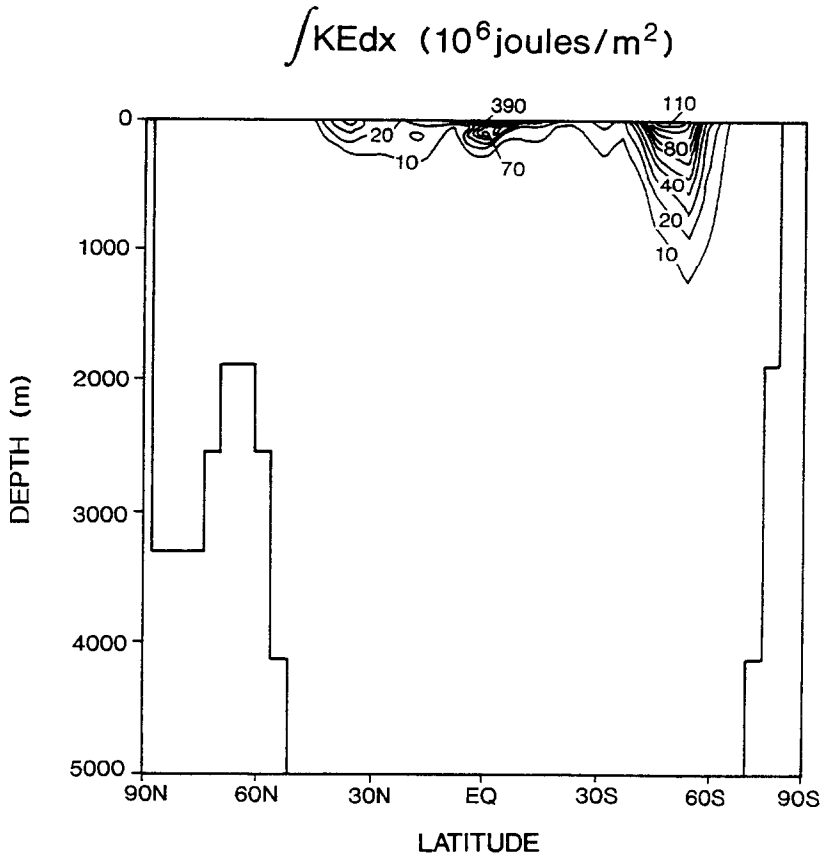

Fig. 8. Zonally integrated kinetic energy (10^6 J m^{-2}) for the mean circulation as derived from a coarse-resolution (nominally 4 × 4°) ocean GCM (after Toggweiler, 1994).

At our 6°W section, located some 2000 km downstream of the South Georgia plateau, the input of dissolved Fe and particulate Fe and Al still can be seen (Figs 9–11). Similarly, in a 140°W section of the Equatorial Pacific Ocean, the Equatorial Undercurrent is discernible from the enhanced dissolved Fe and particulate Al (Coale *et al.*, 1996), presumably derived from its shelf sources some 6000 km upstream in the western Pacific margin (off New Guinea). This undercurrent also represents a considerable amount of kinetic energy (Fig. 8), albeit less than the Antarctic Polar Front.

The distribution of total particulate Al (as measured independently on a separate set of samples) serves as the most convincing evidence of terrestrial input into the Polar Front (Fig. 9). For both transects 5/6 and 11, distinct particulate Al maxima of ~10–15 nM are observed at the Polar Frontal region as well as ~6–10 nM at the AWB front, which, during the final section 11, largely coincided with the MIZ of retreating sea-ice. The total particulate Al concentrations in the regions of the Polar Front and the AWB/MIZ are of the same order in both transects, which means that the magnitude of particle import in both transects remains fairly uniform in place and time. The AWB at 6°W is considered the eastward extension of the aforementioned Weddell–Scotia Confluence where at 49°W, i.e.

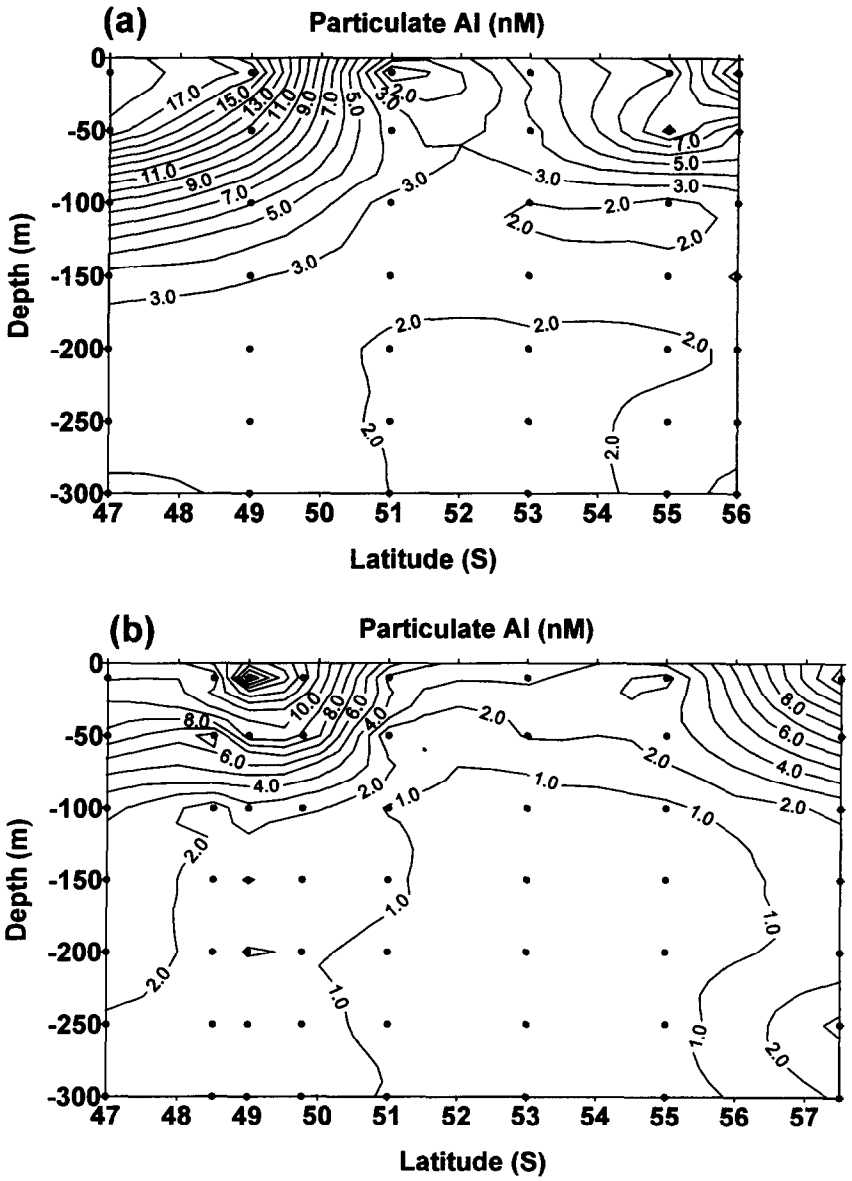

Fig. 9. Section plots of total particulate Al distributions determined by F. Dehairs. Both sections have distinct maxima at the Polar Frontal region (PF) and the MIZ in the region of the southern ACC Front and the AWB. (a) Section plot of combined transect 5 and 6. PF: north of 50.5°S; MIZ: from 55.5°S southward. (b) Section plot of transect 11. PFZ: between 48°S and 51°S; MIZ at about 58°S overlying the AWB.

some 43° longitude closer to the extensive shelves of the Antarctic Peninsula region, both the particulate Al (Dehairs *et al.*, 1992) and dissolved Fe (Nolting *et al.*, 1991) are higher. Using the given Al values (Fig. 9) and a molar crustal abundance ratio of Fe/Al = 0.33 (Taylor, 1964) the calculated particulate Fe distributions would be from 0.5 to 1 nM in the open

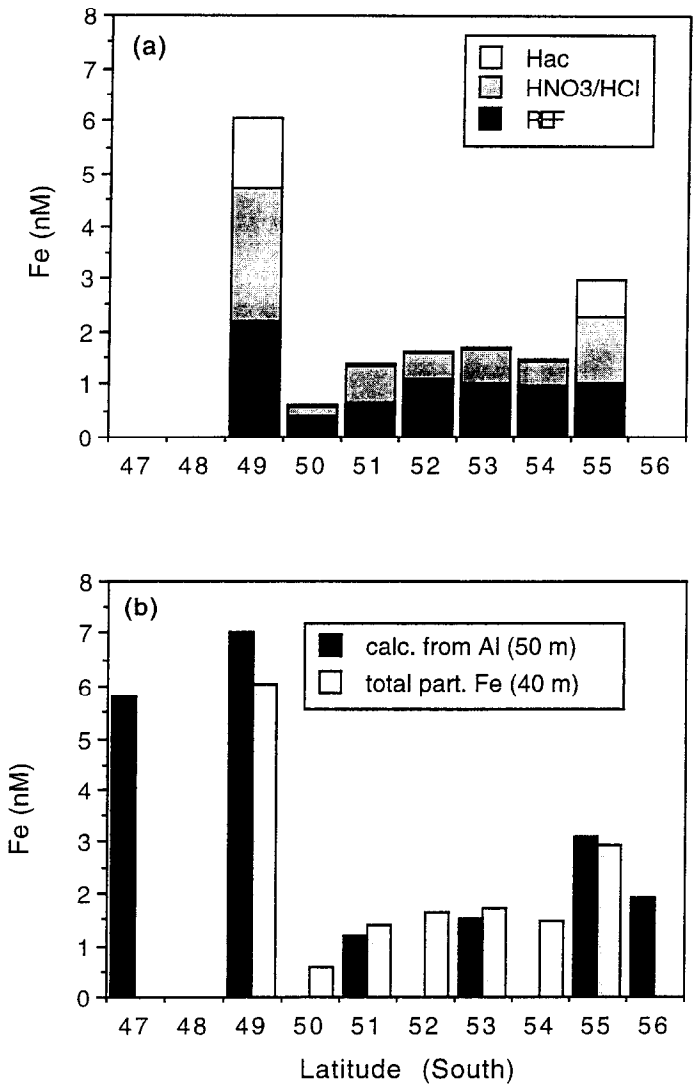

Fig. 10. (a) Sequential chemical leached particulate Fe fractions at 40 m depth during transect 5 as measured by GFAAS. Acetic acid leach (white), nitric/hydrochloric leach (grey) and refractory residual (black). (b) Comparison of the sum of above three particulate Fe fractions at 40 m depth with calculated total particulate Fe from the independently sampled and measured total particulate Al at 50 m depth, using the molar crustal abundance ratio Fe/Al of 0.33 (Taylor, 1964).

Southern ACC waters and as high as 6 nM and up to 5 nM in the Polar Frontal region and in the AWB/MIZ, respectively.

The measured total particulate Fe concentrations at 40 m depth in transect 5 (Fig. 10a) support the above calculations on the basis of measured Al at 50 m depth (Fig. 9a). The sample taken at 49°S in the Polar Frontal region has the highest particulate Fe concentration, 6.0 nM, whereas in the southern ACC waters the particulate Fe

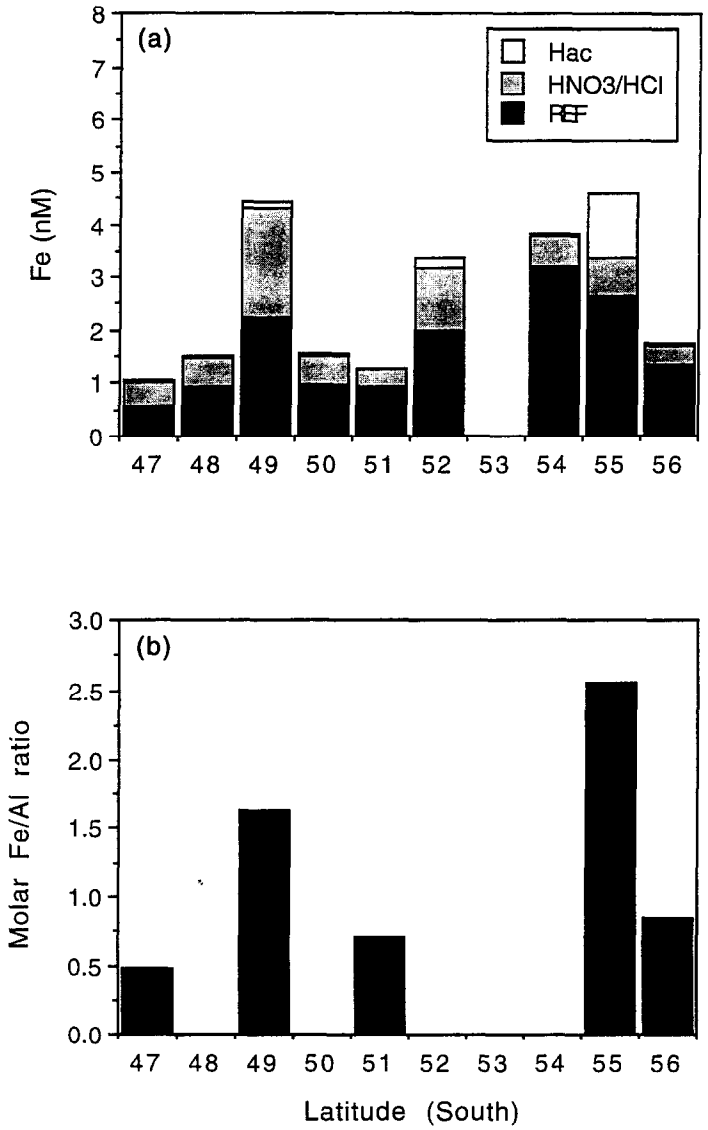

Fig. 11. (a) Sequential chemical leached particulate Fe at 200 m depth of transect 5. (b) The observed Fe/Al ratio at 200 m depth of transect 5 using the total particulate Fe measured at NIOZ and total particulate Al determined by F. Dehairs. Additional results of particulate metals will be reported elsewhere. At 48°S, 50°S, 52°S and 54°S no ratio is given as there is no corresponding Al value available.

concentration varies from 0.6 nM to 1.7 nM. This good agreement of the measured total particulate Fe data at 40 m depth with the calculated particulate Fe data from the Al data at 50 m depth is shown in Fig. 10b. The leachable fraction (which is conceivably more easily available for biota) at the Polar Front (49°S) and the southern ACC Front (~55°S) represents 22% of the total particulate Fe, as compared to only 2 or 3% of the particles in the intermediate Southern ACC waters (Fig. 10a).

At 200 m depth (Fig. 11a) the particulate Fe maxima can still be observed in the two fronts at 49°S and 54–55°S, with lower abundances in between, except for an anomalously high value at 52°S that cannot be explained. In between the fronts, the calculated molar Fe/Al ratio at 200 m depth (Fig. 11b) for total material is about 0.48–0.71. For the refractory Fe only, versus total Al, the ratio is lower at 0.25–0.52, comparable to the global average of 0.33 for crustal abundance (Taylor, 1964). However at the fronts, the total ratio attains values of 2.56 in the southern ACC Front and 1.63 in the Polar Frontal region, whereas the refractory Fe versus total Al yields ratios of about 1.47 and 0.83, respectively. The average molar crustal abundance ratio of 0.33 appears to be a minimum average value for marine particles, as marine biogenic Fe fractions and marine authigenic Fe-oxide coatings would not be included. For example Westerlund and Öhman (1991) found in the Weddell Sea a molar ratio Fe/Al = 0.76.

The removal of dissolved Fe from surface waters during eastward transport likely occurs by its incorporation into biogenic particles. Without any new input, the dissolved Fe is expected to decrease eastward as well as with the ongoing season of biological growth. We do not have such an east–west section at the latitude of the Polar Frontal region. However, the east–west transect 1 at 55–57°S in the southern ACC branch provides a small dataset beyond the Sandwich Islands where such a decrease may be discerned tentatively for the upper water samples at 40 m depth (Fig. 12). The trend is still observable down to about 100 m depth, albeit barely, and in fact reverses at 200–300 m depth. Obviously more detailed sampling in an east–west direction along the Polar Front itself is required to resolve the expected lateral trends.

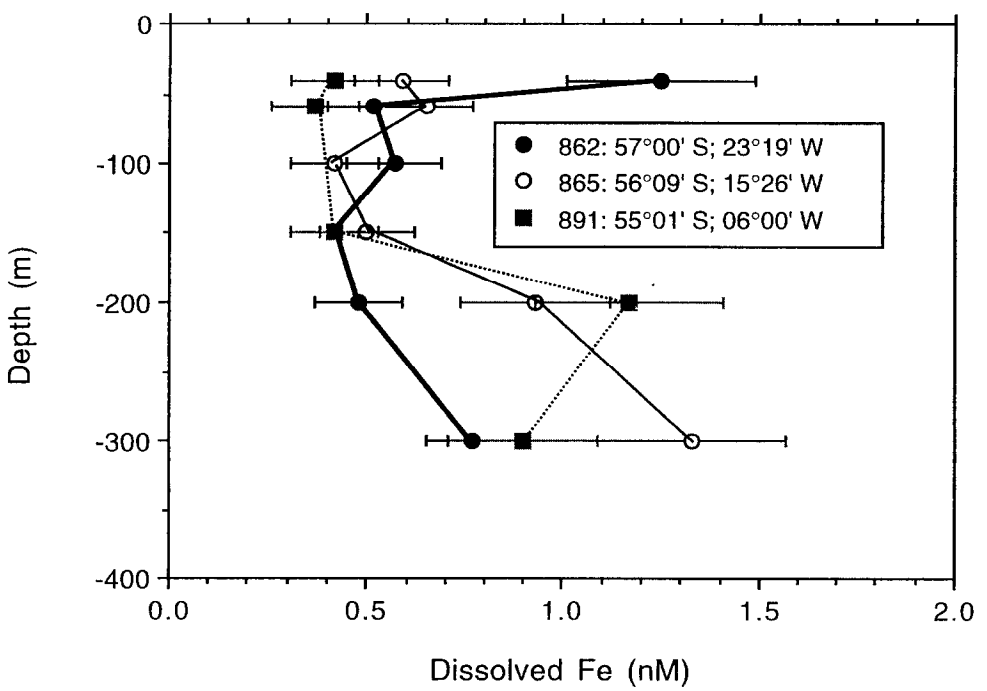

Fig. 12. Vertical profiles in the upper 400 m of dissolved Fe along the east–west transect.

In summary, the major supply of dissolved Fe to surface waters of the offshore Antarctic Ocean appears to be upwelling and mixing from underlying deep waters. In nearshore water, overlying the continental shelf and slope, there is an input from sediment sources. Frontal systems with often rapidly flowing jets such as the Polar Front may bring this signal towards the open ocean, giving rise to local bands of elevated dissolved Fe concentrations. Such bands were observed in the Polar Front and, to a lesser extent, in the southern ACC Front and the AWB. Alternatively aeolian input has been suggested to be important in subAntarctic waters of the Polar Frontal Zone (PFZ), including the Polar Front itself.

SOURCES OF IRON FOR DEEP WATERS

The generally higher input of both dissolved and particulate Fe has been discussed for the energetic Polar Front. The more southern part of the ACC is less but still quite energetic (Fig. 8) and also has been flowing over shoaling seafloor topography of the Sandwich Islands arc ($\sim$28°W), which is the largely submerged connection between the South Georgia and South Orkneys plateaus. In other words the ACC simply has to flow over one or the other of these shallows where exchange with the underlying sediments is inevitable. Subsequently the general upwelling provides a vehicle for bringing dissolved Fe to the surface in the southern ACC branch where dissolved Fe was found to be $\sim$0.31–0.48 nM.

Further west the deep and surface waters of Pacific origin are expected to be more pristine, consistent with the somewhat lower dissolved Fe concentrations of about 0.1–0.76 nM in Drake Passage (63–65°W; Martin *et al.*, 1990a) and the very uniform $\sim$0.2 nM recently encountered at a Pacific Antarctic section at about 90°W, where occasionally values as low as 0.1 nM were observed in the oligotrophic upper water column (de Jong and de Baar, unpublished results). For other remote and oligotrophic oceans, one encounters deep-water dissolved Fe at concentrations between 0.6 and 0.7 nM for station "Papa" (Martin *et al.*, 1989) and between 0.2 and 0.6 nM for the central North Pacific (Bruland *et al.*, 1994).

Another Fe source for the deep ocean basins is volcanic input. It is evident that the Mid-Atlantic Ridge experiences local episodes of volcanic activity. Dissolved Fe(II) emanates in strongly reducing hydrothermal solutions (von Damm *et al.*, 1985a,b; Hudson *et al.*, 1986; Campbell *et al.*, 1988). However, upon mixing with ambient seawater, the immediate and massive precipitation of Fe-sulphides and oxyhydroxides (Edmond *et al.*, 1979; Suter Bowers *et al.*, 1985; Feely *et al.*, 1991; German *et al.*, 1991; Klinkhammer *et al.*, 1994) leads to deposition of metalliferous sediments at the ridge crest. Hence very little dissolved Fe is discernible once the plume is a few miles away from the ridge axis source. Intense tectonic activity is evident from earthquake epicentres at the section across the Mid-Atlantic Ridge and American–Antarctic Ridge (Drumed *et al.*, 1989–90). Vertical profiles of dissolved Fe at two stations within 80 miles from each other show maxima of more than 4 nM dissolved Fe at the isopycnals 27.81–27.83 kg m^{-3} at about 2000 m depth (Fig. 13). This observation is supported by the profile of total dissolvable Fe at station 951 at 52°01'S, 06°01'W, which also shows an Fe maximum at the same isopycnal (Fig. 13). Most remarkably these density surfaces tend to coincide with the ridge crest topography (not shown). It is tempting to attribute the Fe maxima to hydrothermal input derived directly from active sites (Fig. 1). However, judging from the aforementioned rapid removal of Fe in plumes observed elsewhere (Edmond *et al.*, 1979; Suter Bowers *et al.*, 1985; Feely *et al.*, 1991; German *et al.*, 1991; Klinkhammer *et al.*, 1994), it is more likely that the here observed maxima are

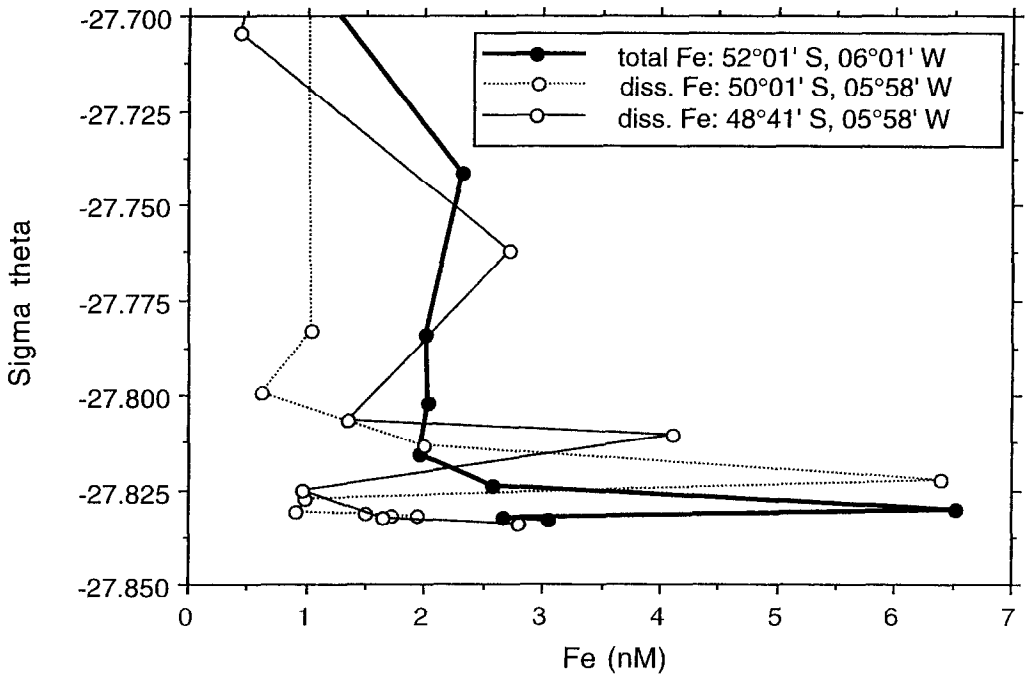

Fig. 13. Three Fe profiles which may be indicative of direct hydrothermal input in the 27.81–27.83 kg m^{-3} isopycnal at about 2000 m depth. The 27.83 kg m^{-3} isopycnal interacts with the ridge crests of the Atlantic–Antarctic Ridge (not shown).

indirectly derived from hydrothermal sources, via the diagenetic mobilisation and current resuspension of metalliferous sediments into nepheloid layers.

DISCUSSION

Where Fe is conceivably a limiting factor of phytoplankton growth and concomitant drawdown of CO_2 from the atmosphere, the now documented high Fe concentrations in the Polar Frontal region provide more favourable conditions for spring diatom blooms. The size-fractionated primary production (Jochem *et al.*, 1995) show that the ~10-fold higher rate of photosynthesis in the Polar Frontal region can be largely ascribed to the >20 μm size class of large diatoms. The more favourable light conditions at the Polar Frontal region would affect all size classes of algae, but the smaller nanoplankton is rapidly consumed in the microbial foodweb (Detmer and Bathmann, 1997), whereas the large diatoms apparently are favoured, both by an abundant supply of iron and by a virtual absence of larger grazers (Dubischar and Bathmann, 1997). As a result, the chlorophyll *a* at transect 11 has a mean value of 1.33 μg dm^{-3} in the upper 120 m of the Polar Frontal region, compared to 0.24 μg dm^{-3} in the southern ACC branch (Bathmann *et al.*, 1997). At the earlier transect 5 (not shown) these mean values were 0.74 μg dm^{-3} in the Polar Frontal region and 0.25 μg dm^{-3} in the southern ACC front (Bathmann *et al.*, 1997). During these two transects, with a time difference of about 18 days, wind stress decreased while daylength

increased, leading to an increase in surface water (upper 40 m) temperature of 1°C. The related decrease of vertical mixing depth (Jochem *et al.*, 1995), together with the increased insolation, are key factors for phytoplankton growth and have led to the spring diatom bloom in the Polar Frontal region. Thus iron supply may yield so-called "pulse areas" of biological productivity, provided there is a rare calm window for plankton growth in the stormy climate of the Antarctic.

The integrated decrease of Fe between these two transects may be due to natural variability in the eddy structure of an active frontal system, but otherwise is consistent with net uptake of iron by plankton particles. Based on two data points in the upper 120 m at each station, the net decrease was 0.73 nM in the Polar Frontal region compared to 0.18 nM in the southerly ACC branch waters. At 100 m depth in the Polar Frontal region, 0.5–2.0 nM Fe disappeared within about 18 days between these two transects.

Between 53° and 55°S, in the vicinity of the southern Front of the ACC, the concentration of dissolved Fe in the upper 150 m increased during the 18 days between transect 5 and 11, from 0.5 to 1.0 nM. This increase may explain the slightly elevated chlorophyll *a* content of 0.3 $\mu g\, l^{-1}$ (Bathmann *et al.*, 1997). The latter is partly accounted for by the occurrence of diatom *Nitzschia prolongatoides* at 54–55°S in section 11. This algae is known to live within or near the sea-ice, and its abundance in open waters would suggest a recent ice-edge melting in the region. This melting event may have given rise to the observed increase of Fe as well.

Recently, Perisinotto *et al.* (1992) reported in the vicinity of the Bouvet and South Sandwich Islands a chlorophyll *a* increase of 3–4 times over off-shore stations. In retrospect, one possible explanation is Fe input from the islands themselves and the surrounding shallow sediments. This is corroborated by recent observations downstream of the Galapagos plateau (Martin *et al.*, 1994). Iron enrichment experiments during our cruise (van Leeuwe *et al.*, 1997; Scharek *et al.*, 1997) also demonstrated that Fe stimulates primary productivity in Antarctic fronts.

The fact that natural Fe supply is adequate to sustain at least some primary production is now reported for many Antarctic regions and seasons: for the Weddell–Scotia Confluence frontal zone in late spring and summer (de Baar *et al.*, 1989, 1990; Buma *et al.*, 1991; Nolting *et al.*, 1991), for the Ross Sea in summer (Martin *et al.*, 1990b) when properly interpreted (Dugdale and Wilkerson, 1990; Banse, 1991), and for the southern branch of the ACC where upwelling supply of dissolved iron is adequate for sustaining moderate levels of primary productivity in a recycling ecosystem of small plankton species. Here we have shown, from comparison of latter southern ACC waters with the Fe-enriched Polar Frontal region, that additional Fe is required for diatom blooms large enough to affect geochemical budgets and fluxes of CO_2 (Bakker *et al.*, 1997) and major nutrients nitrate, phosphate (de Baar *et al.*, 1997) and silicate (Quéguiner *et al.*, 1997) in surface waters (de Baar *et al.*, 1995). The large scale fluxes of major elements C, N, P and Si are a key issue in the Joint Global Ocean Flux Study. In the modern Antarctic Ocean these fluxes apparently are largely driven by light climate in combination with availability of iron, the latter factor hypothesised previously for ancient Antarctic oceans (Martin, 1990). From these observations, it appears that modern Antarctic fronts and nearshore waters are sites of Fe-stimulated productivity, whereas previously natural Fe stimulation was deemed to be rather trivial (Martin and Fitzwater, 1988; Martin *et al.*, 1990b; Laubscher *et al.*, 1993) for the Southern Ocean.

Acknowledgements—We are grateful to Victor Smetacek who gave us the opportunity to join this excellent cruise onboard the R.V. *Polarstern*. The enthusiastic support by officers, engineers and crew has been essential for our

work. We wish to thank Sven Ober and Ronald de Koster for the skilled operation of the CTD, as well as Karel Bakker and Peter Fritsche for the analyses of nutrients. We thank Robby Toggweiler for providing his KE plot as well as fruitful comments. We are grateful to Rob Nolting, Véronique Schoemann and especially Paul Saager for their constructive comments on an earlier version of the manuscript. Various suggestions by the external reviewers, guest editor Michael van der Loeff and editor John Milliman have led to major improvements in the manuscript. This research was supported by grants from the Commissie Antarctisch Onderzoek and the Nederlandse Organisatie voor Wetenschappelijk Onderzoek (NWO) and a graduate student fellowship from NWO/GOA to the first author. This is NIOZ contribution number 3041.

REFERENCES

de Baar H. J. W. (1994) von Liebig's Law of the minimum and plankton ecology (1899–1991). *Progress in Oceanography*, **33**, 347–386.

de Baar H. J. W., A. G. J. Buma, G. Jacques, R. F. Nolting and P. J. Tréguer (1989) Trace metals—iron and manganese effects on phytoplankton growth. *Berichte zur Polarforschung*, **65**, 34–44.

de Baar H. J. W., A. G. J. Buma, R. F. Nolting, G. C. Cadeé, G. Jacques and P. J. Tréguer (1990) On iron limitation of the Southern Ocean: experimental observations in the Weddell and Scotia Seas. *Marine Ecology Progress Series*, **65**, 105–122.

de Baar H. J. W., P. M. Saager, R. F. Nolting and J. van der Meer (1994) Cadmium versus phosphate in the world ocean. *Marine Chemistry*, **46**, 261–281.

de Baar H. J. W., J. T. M. de Jong, D. C. E. Bakker, B. M. Löscher, C. Veth, U. Bathmann and V. Smetacek (1995) Importance of iron for plankton blooms and carbon dioxide drawdown in the Southern Ocean. *Nature*, **373**, 412–415.

de Baar H. J. W., M. A. van Leeuwe, R. Scharek, L. Goeyens, K. M. J. Bakker and P. Fritsche (1997) Nutrient anomalies in *Fragilariopsis kerguelensis* blooms. Iron deficiency and the nitrate/phosphate ratio (A. C. Redfield) of the Antarctic Ocean. *Deep-Sea Research II*, **44**, 229–260.

Bakker D. C. E., H. J. W. de Baar and U. V. Bathmann (1997) Changes of carbon dioxide in surface waters during spring in the Southern Ocean. *Deep-Sea Research II*, **44**, 91–127.

Balistrieri L., P. G. Brewer and J. W. Murray (1981) Scavenging residence times of trace metals and surface chemistry of sinking particles in the deep ocean. *Deep-Sea Research*, **28**, 101–121.

Banse K. (1991) Iron availability, nitrate uptake, and exportable new production in the subarctic Pacific. *Journal of Geophysical Research*, **96**(C1), 741–748.

Bathmann U. V., R. Scharek, C. Klaas, C. D. Dubischar and V. Smetacek (1997) Spring development of phytoplankton biomass and composition in major water masses of the Atlantic sector of the Southern Ocean during austral spring. *Deep-Sea Research II*, **44**, 51–67.

van den Berg C. M. G. (1995) Evidence for organic complexation of iron in seawater. *Marine Chemistry*, **50**, 139–157.

Boyle E. A., F. R. Sclater and J. M. Edmond (1976) On the marine geochemistry of cadmium. *Nature*, **263**, 42–44.

Boyle E. A., F. R. Sclater and J. M. Edmond (1977) The distribution of dissolved copper in the Pacific. *Earth and Planetary Science Letters*, **37**, 38–54.

Boyle E. A., S. S. Huested and S. P. Jones (1981) On the distribution of copper, nickel and cadmium in the surface waters of the north Atlantic and north Pacific Ocean. *Journal of Geophysical Research*, **86**, 8048–8066.

Brand L. (1991) Minimum iron requirements of phytoplankton and the implications for the biogeochemical control of new production. *Limnology and Oceanography*, **36**, 1756–1771.

Broecker W. S. (1981) Geochemical tracers and ocean circulation. In: *Evolution of physical oceanography*, B. A. Warren and C. Wunsch, editors, The MIT Press, Cambridge, MA, 460 pp.

Bruland K. W. (1980) Oceanographic distributions of cadmium, zinc, nickel, and copper in north Pacific. *Earth and Planetary Science Letters*, **47**, 176–198.

Bruland K. W. and R. P. Franks (1979) Sampling and analytical methods for the determination of copper, cadmium, zinc, and nickel at the nanogram per liter level in sea water. *Analytica Chimica Acta*, **105**, 233–245.

Bruland K. W. and R. P. Franks (1983) Manganese, nickel, copper, zinc and cadmium in the western north Atlantic. In: *Trace metals in sea water*, C. S. Wong, E. Boyle, K. Bruland, J. D. Burton and E. D. Goldberg, editors, Plenum Press, New York, pp. 395–413.

Bruland K. W., G. A. Knauer and J. H. Martin (1978a) Cadmium in northeast Pacific waters. *Limnology and Oceanography*, **23**, 618–625.

Bruland K. W., G. A. Knauer and J. H. Martin (1978b) Zinc in northeast Pacific water. *Nature*, **271**, 741–743.

Bruland K. W., K. J. Orians and J. P. Cowen (1994) Reactive trace metals in the stratified central North Pacific. *Geochimica et Cosmochimica Acta*, **58**, 3171–3182.

Buma A. G. J., H. J. W. de Baar, R. F. Nolting and A. J. van Bennekom (1991) Metal enrichment experiments in the Weddell–Scotia Seas: effects of iron and manganese on various plankton communities. *Limnology and Oceanography*, **36**, 1865–1878.

Byrne R. H., L. R. Kump and K. J. Cantrell (1988) The influence of temperature and pH on trace metal speciation in seawater. *Marine Chemistry*, **25**, 163–181.

Campbell A. C., M. R. Palmer, G. P. Klinkhammer, T. S. Bowers, J. M. Edmond, J. R. Lawrence, J. F. Casey, G. Thompson, S. Humphris, P. Rona and J. A. Karson (1988) Chemistry of hot-springs on the Mid-Atlantic Ridge. *Nature*, **335**, 514–519.

Chereskin B. M. and P. A. Castelfranco (1982) Effects of iron and oxygen on chlorophyll biosynthesis. *Plant Physiology*, **68**, 112–116.

Coale K. H., S. E. Fitzwater, R. M. Gordon, K. S. Johnson and R. T. Barber (1996) Control of community growth and export production by upwelled iron in the equatorial Pacific Ocean. *Nature*, **379**, 621–624.

Cullen J. J. (1991) Hypotheses to explain high-nutrient conditions in the open sea. *Limnology and Oceanography*, **36**, 1578–1599.

Cullen J., X. Yang and H. L. Macintyre (1992) Nutrient limitation and marine photosynthesis. In: *Primary production and biochemical cycles in the sea*. P. G. Falkowski and A. D. Woodhead, editors, Plenum Press, New York, pp. 69–89.

Cunningham W. C. and W. H. Zoller (1981) The chemical composition of remote area aerosols. *Journal of Aerosol Science*, **12**, 367–384.

von Damm K. L., J. M. Edmond, B. Grant, C. I. Measures, B. Walden and R. F. Weiss (1985) Chemistry of submarine hydrothermal solutions at 21°N, East Pacific Rise. *Geochimica et Cosmochimica Acta*, **49**, 2197–2220.

von Damm K. L., J. M. Edmond, C. I. Measures and B. Grand (1985) Chemistry of submarine hydrothermal solutions at Guaymas Basin Gulf of California. *Geochimica et Cosmochimica Acta*, **49**, 2221–2237.

Dehairs F., L. Goeyens, N. Stroobants, P. Bernard, C. Goyet, A. Pisson and R. Chesselet (1990) On suspended barite and oxygen minimum in the Southern Ocean. *Global Biogeochemical Cycles*, **4**, 85–102.

Dehairs F., N. Stroobants and L. Goeyens (1991) Suspended barite as a tracer of biological activity in the Southern Ocean. *Marine Chemistry*, **35**, 399–410.

Dehairs F., L. Goeyens, N. Stroobants and S. Mathot (1992) Elemental composition of suspended matter in the Scotia–Weddell Confluence area during spring and summer 1988 (EPOS Leg 2). *Polar Biology*, **12**, 25–33.

Detmer A. E. and U. V. Bathmann (1997) Distribution patterns of autotrophic pico- and nanoplankton and their relative contribution to algal biomass during spring in the Atlantic sector of the Southern Ocean. *Deep-Sea Research II*, **44**, 299–300.

Dick A. L. (1991) Concentrations and sources of metals in the Antarctic Peninsula aerosol. *Geochimica et Cosmochimica Acta*, **55**, 1827–1836.

Drumed A. V., V. N. Ginsar, I. A. Pojata, N. Y. Stepanenko, N. V. Shebalin, V. I. Shumila and D. I. Zhiv Seismological observatories (1989–90). Earthquake epicentres for the period 1911–1980. In: *International geological-geophysical atlas of the Atlantic Ocean*. G. B. Udintsev, editor, IOC (of UNESCO), Min. Geol. USSR, Ac. Sci. USSR, GUGK, USSR Moscow, 101 pp.

Dubischar C. D. and U. V. Bathmann (1997) Grazing impact of copepods and salps on phytoplankton in the Atlantic sector of the Southern Ocean. *Deep-Sea Research II*, **44**, 415–433.

Duce R. A. (1986) The impact of atmospheric nitrogen, phosphorus and iron species on marine biological productivity. In: *The role of air–sea exchanges in geochemical cycling*, P. Buat–Menard, editor, Reidel, Dordrecht, pp. 497–529.

Duce R. A. and N. W. Tindale (1991) Atmospheric transport of iron and its deposition in the ocean. *Limnology and Oceanography*, **36**, 1715–1726.

Duce R. A., P. S. Liss, J. T. Merrill, E. L. Atlas, P. Buat-Menard, B. B. Hicks, J. M. Miller, J. M. Prospero, R. Arimoto, T. M. Church, W. Ellis, J. N. Galloway, L. Hansen, T. D. Jickells, A. H. Knap, K. H. Reinhardt, B. Schneider, A. Soudine, J. J. Tokos, S. Tsunogai, R. Wollast and M. Zhou (1991) The atmospheric input of trace species to the world ocean. *Global Biogeochemistry Cycles*, **5**, 193–259.

Dugdale R. C. and F. P. Wilkerson (1990) Iron addition experiments in the Antarctic: a re-analysis. *Global Biogeochemistry Cycles*, **4**, 13–19.

Edmond J. M., C. Measures, B. Mangum, B. Grant, F. R. Sclater, R. Collier and A. Hudson (1979) On the formation of metal-rich deposits at ridge crests. *Earth and Planetary Science Letters*, **46**, 19–30.

Eicken H. (1992) The role of sea-ice in structuring Antarctic ecosystems. *Polar Biology*, **12**, 3–12.

Feely R. A., J. H. Trefry, G. J. Massoth and S. Metz (1991) A comparison of scavenging of phosphorus and arsenic from seawater by hydrothermal iron oxyhydroxides in the Atlantic and Pacific Oceans. *Deep-Sea Research*, **38**, 617–623.

van Franeker J. A. (1994) Sea-ice cover and icebergs. *Berichte zur Polarforschung*, **135**, 17–22.

Froelich P. N., G. P. Klinkhammer, M. L. Bender, N. A. Luedtke, G. R. Heath, D. Cullen, P. Dauphin, D. Hammond, B. Hartman and V. Maynard (1979) Early oxidation of organic matter in pelagic sediments of the eastern equatorial Atlantic: Suboxic diagenesis. *Geochimica et Gosmochimica Acta*, **43**, 1075–1090.

Frost B. W. (1991) The role of grazing in nutrient-rich areas of the open sea. *Limnology and Oceanography*, **36**, 1616–1630.

Garcon V. C., F. Thomas, C. S. Wong and J. F. Minster (1992) Gaining insight into the seasonal variability of CO_2 at Ocean Station Papa using an upper ocean model. *Deep-Sea Research*, **39**, 921–938.

Gargett A. E. (1991) Physical processes and the maintenance of nutrient-rich euphotic zones. *Limnology and Oceanography*, **36**, 1527–1545.

German C. R., A. C. Campbell and J. M. Edmond (1991) Hydrothermal scavenging at the Mid-Atlantic Ridge: Modification of trace element dissolved fluxes. *Earth and Planetary Science Letters*, **107**, 101–114.

Gordon R. M., J. H. Martin and G. A. Knauer (1982) Iron in northeast Pacific waters. *Nature*, **299**, 611–612.

Gordon A. L., H. W. Taylor and D. T. Georgi (1977) Antarctic oceanic zonation. In: *Polar oceans*, M. J. Durban, editor, Arctic Institute N. America, McGill University, Montreal, pp. 45–67.

Gran H. H. (1931) On the conditions for the production of plankton in the sea. *Rapports et Procès-verbaux des Réunions, Conseil International pour l'exploration de la Mer*, **75**, 37–46.

Hart T. J. (1934) On the phytoplankton of the southwest Atlantic and the Bellingshausen Sea 1929–1931. *Discovery Reports*, **8**, 1–268.

Hart T. J. (1942) Phytoplankton periodicity in Antarctic surface waters. *Discovery Reports*, **21**, 261–365.

Heath G. R. and J. Dymond (1977) Genesis and transformation of metalliferous sediments from the East Pacific Rise, Bauer Deep and Central Basin, northwest Nazca Plate. *Geological Society of American Bulletin*, **88**, 723–733.

Heywood R. B. and J. Priddle (1987) Retention of phytoplankton by an eddy. *Continental Shelf Research*, 7, 937–955.

Hodge V., S. R. Johnson and E. D. Goldberg (1978) Influence of atmospherically transported aerosols on surface ocean water composition. *Geochemistry Journal*, **12**, 7–20.

Holm-Hansen O., S. Z. El-Sayed, G. A. Franceschini and R. L. Cuhel (1977) Primary production and the factors controlling phytoplankton growth in the Southern Ocean. In: *Adaptations within Antarctic ecosystems*, G. A. Llano, editor, Gulf Publ. Co., Houston, TX, pp. 11–50.

Hong H. and D. R. Kester (1986) Redox state of iron in the offshore waters of Peru. *Limnology and Oceanography*, **31**, 512–524.

Hudson R. J. and F. M. M. Morel (1993) Trace metal transport by marine microorganisms: Implications of metal coordination kinetics. *Deep-Sea Research I*, **40**, 129–150.

Hudson A., M. L. Bender and D. W. Graham (1986) Iron enrichments in hydrothermal plumes over the East Pacific Rise. *Earth and Planetary Science Letters*, **79**, 250–254.

Jochem F. J., S. Mathot and B. Quéguiner (1995) Size fractionated primary production in the open Southern Ocean in Austral spring 1992. *Polar Biology*, **15**, 381–392.

de Jong J. T. M., B. M. Löscher and H. J. W. de Baar (1994) Iron in surface waters and sea-ice in the Antarctic Circumpolar Current. *Abstract in: Eos (Transactions American Geophyscal Union)*, **75**, 178.

Kiørboe T. (1993) Turbulence, phytoplankton cell size, and the structure of pelagic food webs. *Advances in Marine Biology*, **29**, 1–72.

Klinkhammer G., C. R. German, H. Elderfield, M. J. Greaves and A. Mitra (1994) Rare earth elements in hydrothermal fluids and plume particulates by inductively coupled plasma mass spectrometry. *Marine Chemistry*, **45**, 179–186.

Kremling K. and H. Peterson (1978) The distribution of Mn, Fe, Zn, Cd, and Cu in Baltic seawater; a study on the basis of one anchor station. *Marine Chemistry*, **6**, 155–170.

Kumar N., R. F. Anderson, R. A. Mortlock, P. N. Froelich, P. Kubik, B. Dittrich-Hannen and M. Suter (1995)

Increased biological productivity and export production in the glacial Southern Ocean. *Nature*, **378**, 675–680.

Lancelot C. S., S. Mathot, C. Veth and H. J. W. de Baar (1993) On the factors controlling phytoplankton ice edge blooms in the marginal ice zone of the northwestern Weddell Sea during sea ice retreat 1988. *Polar Biology*, **13**, 377–387.

Landing W. M. and K. W. Bruland (1987) The contrasting biogeochemistry of iron and manganese in the Pacific Ocean. *Geochimica et Cosmochimica Acta*, **51**, 29–43.

Laubscher R. K., R. Perisinotto and C. D. Mcquaid (1993) Phytoplankton production and biomass at frontal zones in the Atlantic sector of the Southern Ocean. *Polar biology*, **13**, 471–481.

Ledwell J. R., A. J. Watson and C. S. Law (1993) Evidence for slow mixing across the pycnocline from an open-ocean tracer-release experiment. *Nature*, **364**, 701–703.

van Leeuwe M. A., R. Scharek, H. J. W. de Baar, J. T. M. de Jong and L. Goeyens (1997) Iron enrichment experiments in the Southern Ocean: physiological responses of plankton communities. *Deep-Sea Research II*, **44**, 189–207.

Lewis B. L. and W. M. Landing (1991) The biochemistry of manganese and iron in the Black Sea. *Deep-Sea Research*, **38**, 773–803.

Martin J. H. (1990) Glacial–interglacial CO_2 change: the iron hypothesis. *Paleoceanography*, **5**, 1–13.

Martin J. H. (1991) Iron, Liebig and the greenhouse. *Oceanography*, **4**, 52–55.

Martin J. H. (1992) Iron as a limiting factor in oceanic productivity. In: *Primary productivity and biogeochemical cycles in the sea*, P. G. Falkowski and A. D. Woodhead, editors, Environmental Science Research, Plenum Press, New York, **43**, pp. 123–137.

Martin J. H. and R. M. Gordon (1988) Northeast Pacific iron distributions in relation to phytoplankton productivity. *Deep-Sea Research*, **35**, 177–196.

Martin J. H. and S. E. Fitzwater (1988) Iron deficiency limits phytoplankton growth in the northeast Pacific subarctic. *Nature*, **331**, 341–343.

Martin J. M. and M. Meybeck (1979) Elemental mass balance of material carried by major world rivers. *Marine Chemistry*, **7**, 173–206.

Martin J. H., R. M. Gordon, S. E. Fitzwater and W. W. Broenkow (1989) VERTEX: phytoplankton/iron studies in the Gulf of Alaska. *Deep-Sea Research*, **36**, 649–680.

Martin J. H., R. M. Gordon and S. E. Fitzwater (1990a) Iron in Antarctic waters. *Nature*, **345**, 156–158.

Martin J. H., S. E. Fitzwater and R. M. Gordon (1990b) Iron deficiency limits phytoplankton growth in Antarctic waters. *Global Biogeochemical Cycles*, **4**, 5–12.

Martin J. H. M., S. E. Fitzwater, R. M. Gordon, G. N. Hunter and S. J. Tanner (1993) Iron, primary productivity and carbon–nitrogen flux studies during the JGOFS Noth Atlantic Bloom Experiment. *Deep-Sea Research II*, **40**, 115–134.

Martin J. H. *et al.* (1994) Testing the iron hypothesis in ecosystems of the equatorial Pacific Ocean. *Nature*, **371**, 123–129.

Miller C. B., B. W. Frost, B. Booth, P. A. Wheeler, M. R. Landry and N. Welschmeyer (1991a) Ecological processes in the subArctic Pacific: Iron limitation cannot be the whole story. *Oceanography*, **4**, 71–78.

Miller C. B., B. W. Frost, P. A. Wheeler, M. R. Landry, N. Welschmeyer and T. M. Powell (1991b) Ecological dynamics in the subArtic Pacific, a possible iron-limited system. *Limnology and Oceanography*, **36**, 1600–1615.

Moore R. M. (1978) The distribution of dissolved copper in the eastern Atlantic Ocean. *Earth and Planetary Science Letters*, **47**, 176–198.

Moore R. M., J. E. Milley and A. Chatt (1984) The potential for biological mobilization of trace elements from aeolian dust in the ocean and its importance in the case of iron. *Oceanologica Acta*, **7**, 221–228.

Morel F. M. M., R. J. Hudson and N. M. Price (1991) Limitation of productivity by trace metals in the sea. *Limnology and Oceanography*, **36**, 1742–1755.

Moum J. N. and T. R. Osborn (1986) Mixing in the Main Thermocline. *Journal of Physical Oceanography*, **16**, 1250–1259.

Murray J. W. and G. Gill (1978) The geochemistry of iron in Puget Sound. *Geochimica et Cosmochimica Acta*, **42**, 9–19.

Nolting R. F., H. J. W. de Baar, A. J. van Bennekom and A. Masson (1991) Cadmium, copper and iron in the Scotia Sea, Weddell Sea and Weddell/Scotia Confluence (Antarctica). *Marine Chemistry*, **35**, 219–243.

Obata H., H. Karatani and E. Nakayama (1993) Automated determination of iron in seawater by chelating resin concentration and chemiluminescence detection. *Analytical Chemistry*, **65**, 1524–1528.

Orsi A. H., T. Whitworth and W. D. Nowlin (1995) On the meridional extent and fronts of the Antarctic Circumpolar Current. *Deep-Sea Research I*, **42**, 641–673.

Perisinotto R., R. K. Laubscher and C. D. Mcquaid (1992) Marine productivity enhancement around Bouvet and South Sandwich Islands (Southern Ocean). *Marine Ecological Progress*, **88**, 41–53.

Peterson R. G. and L. Stramma (1991) Upper-level circulation in the South Atlantic Ocean. *Progress in Oceanography*, **26**, 1–73.

Price N. M., B. A. Ahner and F. M. M. Morel (1994) The equatorial Pacific Ocean: Grazer-controlled phytoplankton populations in an iron-limited ecosystem. *Limnology and Oceanography*, **39**, 520–534.

Prospero J. M. (1981) Eolian transport to the world ocean In: *The sea*, C. Emiliani, editor, John Wiley, Chichester, U.K., Vol. 7, pp. 801–874

Quéguiner B., P. Treguer, I. Peeken and R. Scharek (1997) Biogeochemical dynamics and the silicon cycle in the Atlantic sector of the Southern Ocean during austral spring 1992. *Deep-Sea Research II*, **44**, 69–89.

Raven J. (1988) The iron and molybdenum use efficiencies of plant growth with different energy, carbon and nitrogen sources. *New Phytology*, **109**, 279–287.

Raven J. (1990) Predictions of Mn and Fe use efficiencies of phototrophic growth as a function of light availability for growth and of C assimilation pathway. *New Phytology*, **116**, 1–18.

Riegman R., B. R. Kuipers, A. A. M. Noordeloos and H. J. Witte (1993) Size-differential control of phytoplankton and the structure of plankton communities. *Netherlands Journal of Sea Research*, **31**, 255–265.

Rona P. A., G. Thompson, M. J. Mottl, J. A. Karson, W. J. Jenkins, D. Graham, M. Mallette, K. von Damm and J. M. Edmond (1984) Hydrothermal Activity at the Trans-Atlantic Geotraverse Hydrothermal Field, Mid-Atlantic Ridge Crest at 26°N. *Journal of Geophysical Research*, **89**(B13), 11365–11377.

Rue E. L. and K. W. Bruland (1995) Complexation of iron (III) by natural organic ligands in the North Pacific as determined by a new competitive ligand equilibration/adsorptive cathodic stripping voltammetric method. *Marine Chemistry*, **50**, 117–138.

Russell M. J., R. M. Daniel and A. J. Hall (1993) On the emergence of life via catalytic iron-sulphide membranes. *Terra Nova*, **5**, 343–347.

Rutgers van der Loeff M. M., J. Friedrich and U. V. Bathmann (1997) Carbon export during the Spring Bloom at the Antarctic Polar Front, determined with the natural tracer ^{234}Th. *Deep-Sea Research II*, **44**, 457–478.

Saager P. M., H. J. W. de Baar and P. H. Burkill (1989) Manganese and iron in Indian Ocean waters. *Geochimica et Cosmochimica Acta*, **53**, 2259–2267.

Saager P. M., H. J. W. de Baar and R. J. Howland (1992) Cd, Zn, Ni and Cu in the Indian Ocean. *Deep-Sea Research*, **39**, 9–35.

Sakshaug E. and O. Holm-Hansen (1984) Factors governing pelagic production in polar oceans. In: *Marine phytoplankton and productivity*, O. Holm-Hansen, L. Bolis and R. Gilles, editors, Springer-Verlag, Berlin, pp. 1–18.

Sclater F. R., E. A. Boyle and J. M. Edmond (1976) On the marine geochemistry of nickel. *Earth and Planetary Science Letters*, **31**, 119–128.

Scharek R., M. A. van Leeuwe and H. J. W. de Baar (1997) Responses of Southern Ocean phytoplankton to the addition of trace metals. *Deep-Sea Research II*, **44**, 209–227.

Sholkovitz E. R. (1978) The flocculation of dissolved Fe, Mn, Al, Cu, Ni, Co and Cd during estuarine mixing. *Earth and Planetary Science Letters*, **41**, 77–86.

Smetacek V., H. J. W. de Baar, U. V. Bathmann, K. Lochte and M. M. Rutgers van der Loeff (1997) Ecology and biochemistry of the Antarctic Circumpolar Current during Austral Spring—Results of the JGOFS expedition ANT X/6 aboard R.V. *Polarstern*. *Deep-Sea Research II*, **44**.

Smith Jr, W. O. and E. Sakshaug (1990) Polar phytoplankton. In: *Polar oceanography, Part B, Chemistry, biology and geology*, W. O. Smith Jr, editor, Academic Press, New York, pp. 477–517.

Staley J. T. and G. H. Orians (1992) Evolution and the biosphere. In: *Global biogeochemical cycles*, E. S. Butcher, R. J. Charlson, G. H. Orions and G. V. Wolfe, editors, Academic Press, London, pp. 21–54.

Stumm W. and J. J. Morgan (1981) *Aquatic chemistry*, Wiley & Sons, Chichester, U.K., 780 pp.

Sullivan C. W., K. R. Arrigo, C. R. McClain, J. C. Comiso and J. Firestone (1993) Distributions of phytoplankton blooms in the Southern Ocean. *Science*, **262**, 1832–1837.

Sunda W. G., D. G. Swift and S. A. Huntsman (1991) Low iron requirement for growth in oceanic phytoplankton. *Nature*, **351**, 55–57.

Suter Bowers T., K. L. von Damm and J. M. Edmond (1985) Chemical evolution of mid-ocean ridge hot springs. *Geochimica et Cosmochimica Acta*, **49**, 2239–2252.

Symes J. L. and D. R. Kester (1985) The distribution of iron in the northwest Atlantic. *Marine Chemistry*, **17**, 57–74.

Taylor S. R. (1964) Abundance of chemical elements in the continental crust: a new table. *Geochimica et Cosmochimica Acta*, **28**, 1273–1285.

Taylor S. R. and S. M. McLennan (1985) *The continental crust: Its composition and evolution.* Blackwell Scientific, Oxford, 312 pp.

Tchernia P. (1980) Hydrology of the Southern Ocean. In: *Descriptive regional oceanography*, J. C. Swallow, editor, Pergamon Press, Oxford, pp. 61–85.

Thompson G., S. E. Humphris, B. Schroeder and M. Sulanowska (1988) Active vents and massive sulfides at 26°N (TAG) and 23°N (SNAKEPIT) on the Mid-Atlantic Ridge. *Canadian Mineralogist*, **26**, 697–711.

Timmermans K. R., W. Stolte and H. J. W. de Baar (1994) Iron-mediated effects on nitrate reductase in marine phytoplankton. *Marine Biology*, **121**, 389–396.

Toggweiler J. R. (1994) The ocean's overturning circulation. *Physics Today*, **47**, 45–53.

Trenberth K. E., W. G. Large and J. G. Olson (1990) The mean annual cycle in global ocean wind stress. *Journal of Physical Oceanography*, **20**, 1742–1760.

Veth C., I. Peeken and R. Scharek (1997) Physical anatomy of fronts and surface waters in the ACC near the 6°W meridian during austral spring 1992. *Deep-Sea Research II*, **44**, 23–49.

Wächtershäuser G. (1992) Groundworks for an evolutionary biochemistry; the iron-sulphur world. *Progress in Biophysics and Molecular Biology*, **58**, 85–201.

Wagenbach D., U. Görlach, K. Moser and K. O. Münnich (1988) Coastal Antarctic aerosol: the seasonal pattern of its chemical composition and radionuclide content. *Tellus*, **40B**, 426–436.

Waite T. D., R. Szymczak, Q. I. Espey and M. J. Furnas (1995) Diel variations in iron speciation in northern Australian shelf waters. *Marine Chemistry*, **50**, 79–92.

Walsh J. J. (1976) Herbivory as a factor in patterns of nutrient utilisation in the sea. *Limnology and Oceanography*, **21**, 1–13.

Wells M. L. and L. M. Mayer (1991) Variations in the chemical lability of iron in estuarine, coastal and shelf waters and its implications for phytoplankton. *Marine Chemistry*, **32**, 195–210.

Wells M. L., N. M. Price and K. W. Bruland (1995) Iron chemistry in seawater and its relationship to phytoplankton: a workshop report. *Marine Chemistry*, **48**, 157–182.

Westerlund S. and P. Öhman (1991) Iron in the water column of the Weddell Sea. *Marine Chemistry*, **35**, 199–217.

Wheeler P. A. and S. A. Kokkinakis (1990) Ammonium recycling limits nitrate use in oceanic subarctic Pacific. *Limnology and Oceanography*, **35**, 1267–1278.

Wu J. and G. W. Luther III (1994) Size-fractionated iron concentrations in the water column of the northwest Atlantic ocean. *Limnology and Oceanography*, **39**, 1119–1129.

Zhuang G., R. A. Duce and D. R. Kester (1990) The dissolution of atmospheric iron in surface seawater of the open ocean. *Journal of Geophysical Research*, **95**(C9), 16207–16216.

Zhuang G. Z., Z. Yi, R. A. Duce and P. R. Brown (1992) Chemistry of iron in marine aerosols. *Global Biogeochemical Cycles*, **6**, 161–173.